



Search for $\chi_{cJ} \rightarrow \Lambda \bar{\Lambda} \phi$

Yueming Shen¹, Lin Zhu², Qingping Ji¹, Weimin Song², and Zhiyong Wang³



¹Henan Normal University, Xinxiang

²Jilin University, Changchun

³Institute of High Energy Physics, Beijing

HFP Group, Oct.22, 2020



Outline

- Motivation
- Data Sample
- Event selection
- Background analysis
- Intermediate state
- Systematic uncertainty
- Summary

Motivation

Search for possible excited baryon states consisting of BV

- a) Search for the potential excited baryons, refer to $\psi(3686) \rightarrow \Lambda \bar{\Lambda} \eta$ [1] and $\psi(3686) \rightarrow \Lambda \bar{\Lambda} \omega$ [2].

Search for possible $B\bar{B}$ threshold enhancements

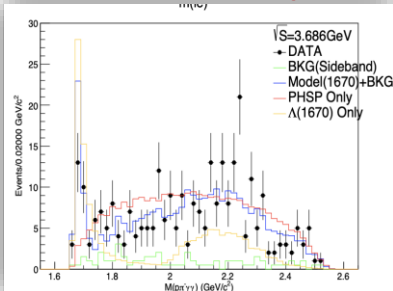
- b) Search for the threshold enhancement in $M_{B\bar{B}}$, refer to $\psi(3686) \rightarrow \Lambda \bar{\Lambda} \omega$ [2] and $\psi(3686) \rightarrow \Lambda \bar{\Lambda} \phi$ [3].

Measure the branching fraction

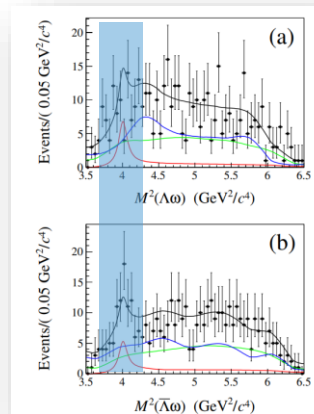
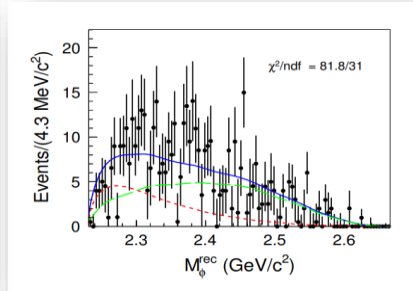
- c) Recently, $\chi_{cJ} \rightarrow B\bar{B}P$ ($\chi_{cJ} \rightarrow \Lambda \bar{\Lambda} \eta$) are observed at BESIII [4],

Similarly, Search for $\chi_{cJ} \rightarrow B\bar{B}V$ decays, such as $\chi_{cJ} \rightarrow \Lambda \bar{\Lambda} \phi$, is interested.

[1] $\psi(3686) \rightarrow \Lambda \bar{\Lambda} \eta$



[3] $\psi(3686) \rightarrow \Lambda \bar{\Lambda} \phi$



[2] $\psi(3686) \rightarrow \Lambda \bar{\Lambda} \omega$



- [1] BAM-00538: Measurement of $\psi(3686) \rightarrow \eta \pi^0 \Lambda \bar{\Lambda}$, by Shi Wang et al.
 [2] BAM-00336, Honghong Zhang et al., Study of Ψ' to $\omega \Lambda \bar{\Lambda}$.
 [3] BAM-00421: Observation of $\psi(3686) \rightarrow \phi \Lambda \bar{\Lambda}$, by Aonan Zhu et al.
 [4] BAM-00496: Observation of $\chi_{cJ} \rightarrow \eta \Lambda \bar{\Lambda}$, by Yijia Zeng et al.

Data samples

Data set	Number of events	BOSS version
09+12 $\psi(3686)$ data	4.48×10^8	709
2021 $\psi(3686)$ data	$\sim 22.6 \times 10^8$ [1]	
09+12 $\psi(3686)$ inclusive MC	5.06×10^8	
2021 $\psi(3686)$ inclusive MC	$\sim 23 \times 10^8$ [2]	
PHSP MC	3 million for each channel (09+12+21)	

[1] C. Liu, Z.Y. Wang et al, Preliminary Result for the Total Number of $\psi(2S)$ Events Taken in 2021, [Online] 16 Jun. 2022 for BESIII Summer Collaboration Meeting in Beijing.

[2] J.S. Luo, R.G. Ping et al, Progress in BesEvtGen, [Online] 13 Jun. 2022 for BESIII Summer Collaboration Meeting in Beijing.

Event selection

Charged tracks

- $|\cos\theta| < 0.93$
- **No vertex constraint**
- $N \geq 6, N_m \geq 3, N_p \geq 3$

$\Lambda(\bar{\Lambda})$ reconstruction :

- 2nd vertex fit
- $\Delta_{\min} = (M_{p\pi^-} - m_{\Lambda})^2 + (M_{\bar{p}\pi^+} - m_{\bar{\Lambda}})^2 \Rightarrow \Lambda_{\min}, \bar{\Lambda}_{\min}$

Particle identification

- For Kaon:
Prob(K) > Prob(p), Prob(K) > Prob(pi)
- $N_{K^+} = N_{K^-} = 1$;
- $|V_z| < 10, |V_{xy}| < 1$

Good photon

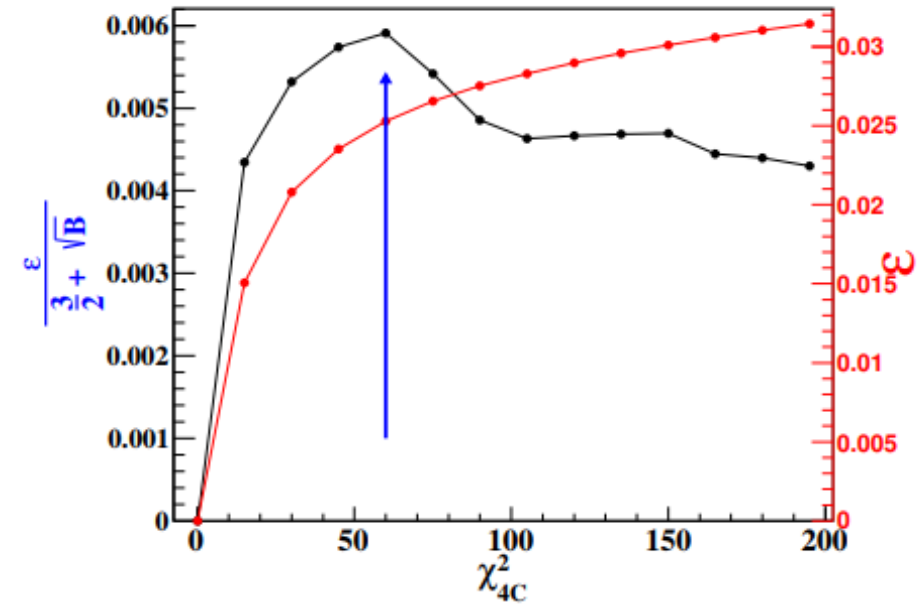
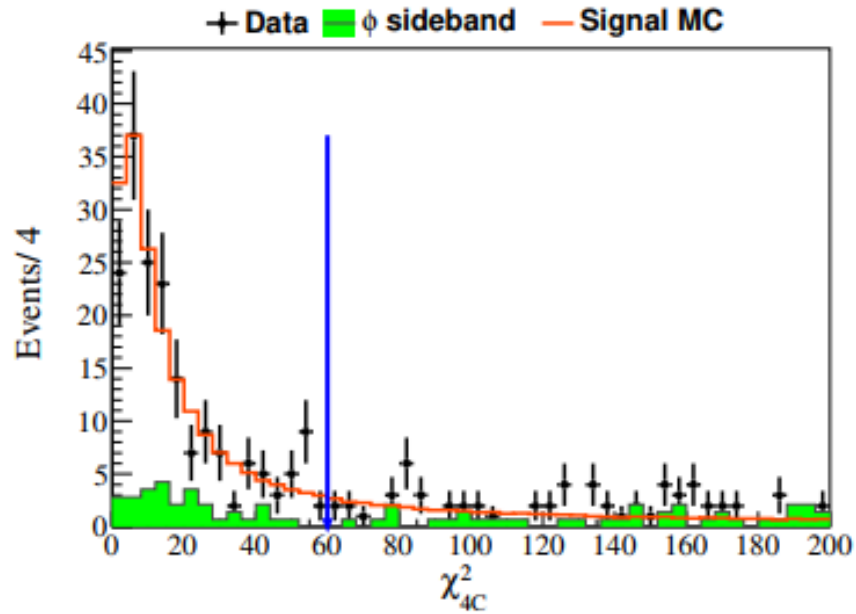
- $0 \leq \text{TDC} \leq 14$
- Barrel : $E > 0.025 \text{ GeV}, |\cos\theta| < 0.8$
- End cap : $E > 0.050 \text{ GeV}, 0.86 < |\cos\theta| < 0.92$
- $N_{\gamma} \geq 1$

4C-kinematic fit with

$$\psi(3686) \rightarrow \gamma \Lambda \bar{\Lambda} K^+ K^-$$

- Four-Constraint (4-C) kinematic fit is performed with $\psi(3686) \rightarrow \gamma \Lambda \bar{\Lambda} K^+ K^-$ hypothesis.

Event selection: 4C kinematic fit

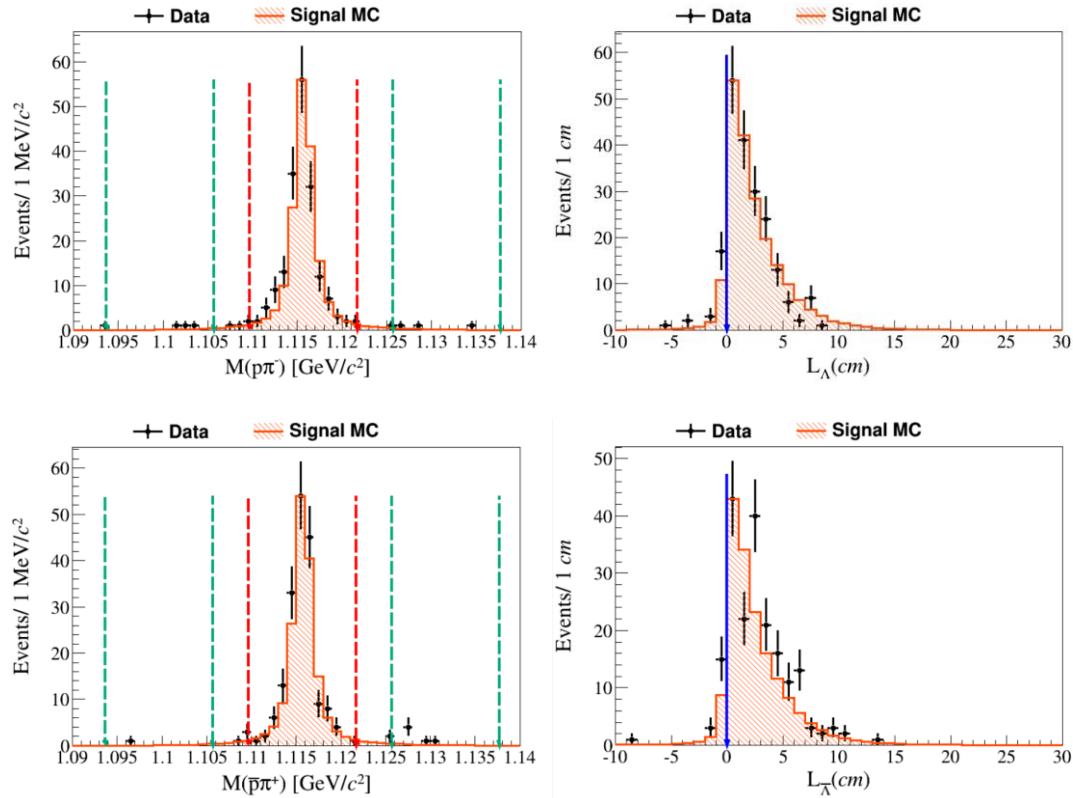


- $\chi^2_{4C}(\gamma\bar{p}p^-K^+K^-\pi^+\pi^-) < 60$

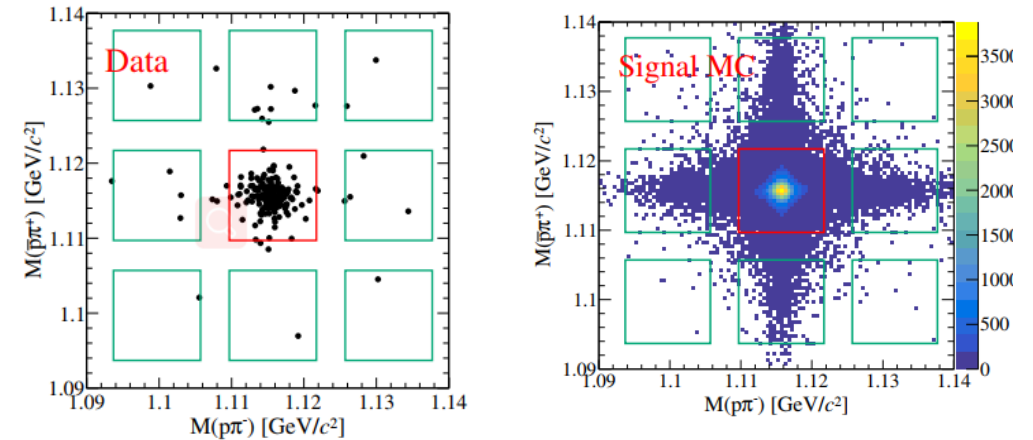
*The green histograms are backgrounds from ϕ .

Event selection:

$M(\Lambda)$ & scatter plot: $M(p\pi^-)$ v.s. $M(\bar{p}\pi^+)$

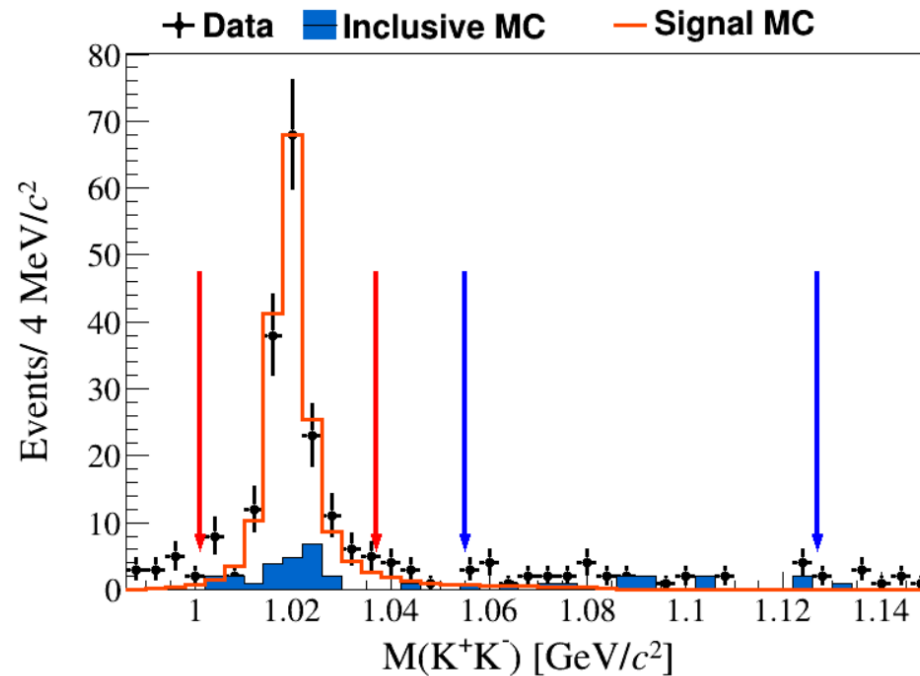


- 1D-Signal region:
 $|M(p\pi^-) - m(\Lambda)| < 6 \text{ MeV}/c^2$
- 1D-Sideband region:
 $10 < |M(p\pi^-) - m(\Lambda)| < 22 \text{ MeV}/c^2$
- $\text{Length}(\Lambda) > 0$ & $\text{Length}(\bar{\Lambda}) > 0$



The sideband events are used to estimate the combinatorial background in the Λ signal region.

Event selection: Mass window of ϕ



- ϕ Signal region:

$$|M(K^+K^-) - m(\phi)| < 0.018 \text{ GeV}/c^2$$

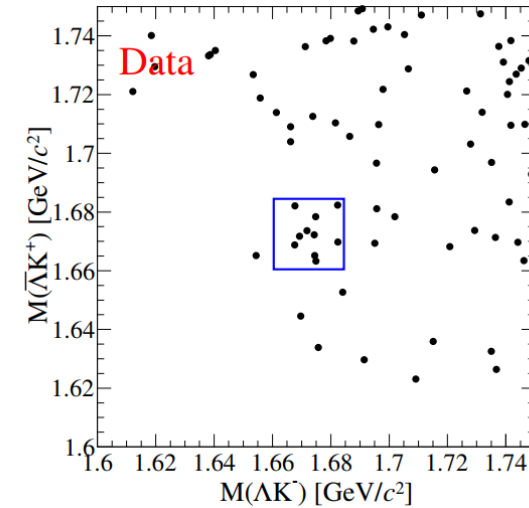
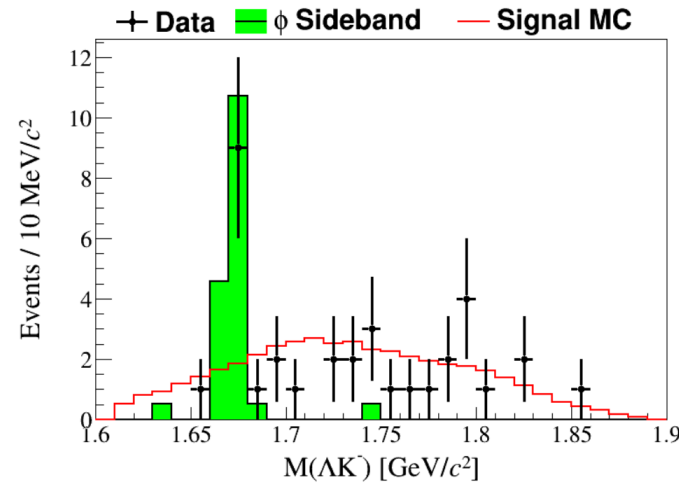
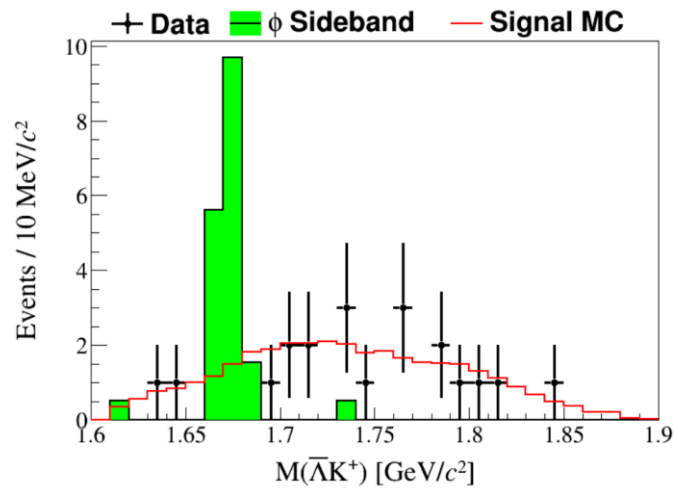
- ϕ Sideband region:

$$1.055 < M(K^+K^-) < 1.127 \text{ GeV}/c^2$$

- We fit the mass spectrum of K^+K^- , $\sigma = 6\text{MeV}$. And a sideband region is selected. Details can be found in the backup.

Further Event selection:

$M(\Lambda K)$ & scatter plot: $M(\bar{\Lambda} K^+) v.s. M(\Lambda K^-)$



● Veto on $\chi_{cJ} \rightarrow \Omega^- \bar{\Omega}^+$:

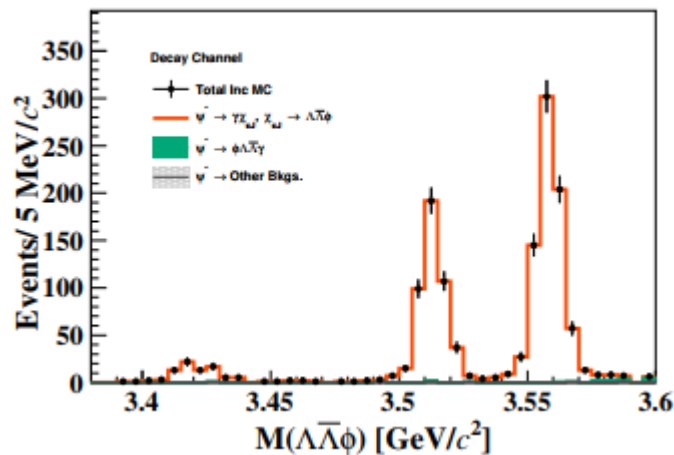
! ($|M(\Lambda K^-) - m(\Omega^-)| < 12 \text{ MeV}/c^2$ && $|M(\bar{\Lambda} K^+) - m(\bar{\Omega}^+)| < 12 \text{ MeV}/c^2$)

Background study

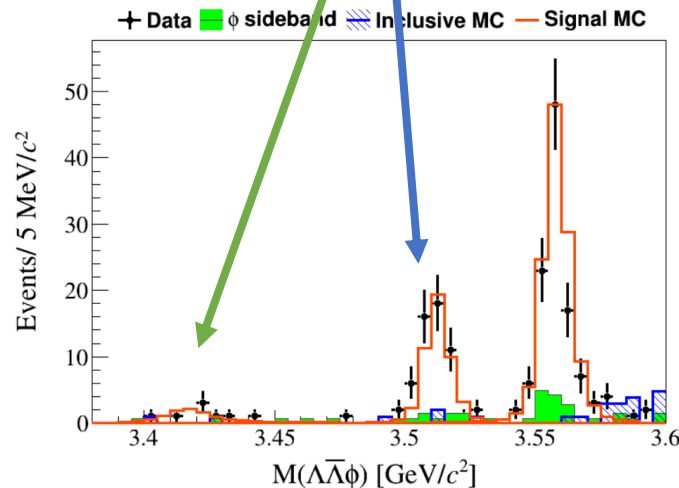
No.	Decay Chain	Final states	nEvt
1	$\psi(3686) \rightarrow \phi \Lambda \bar{\Lambda} \gamma$	$\pi^+ \pi^- K^+ K^- p \bar{p} \gamma$	17
2	$\psi(3686) \rightarrow$ Other backgrounds	...	6



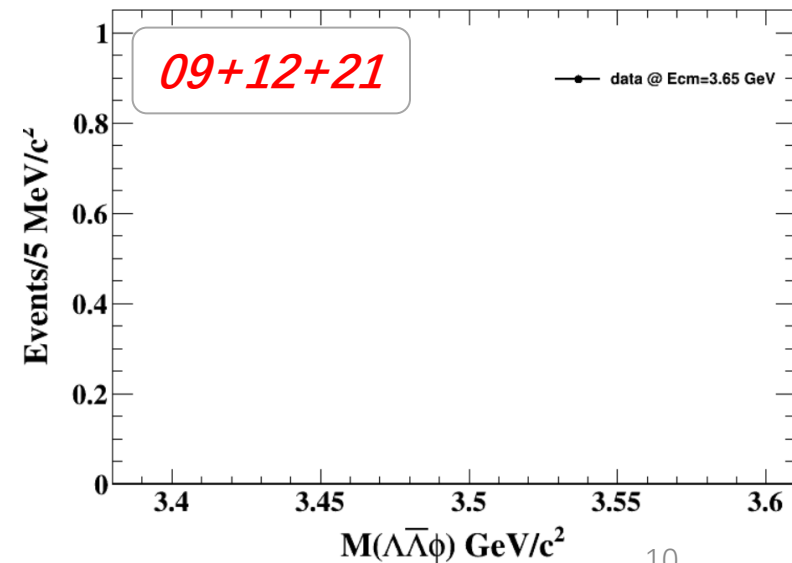
No
peaking background



Signal Channel

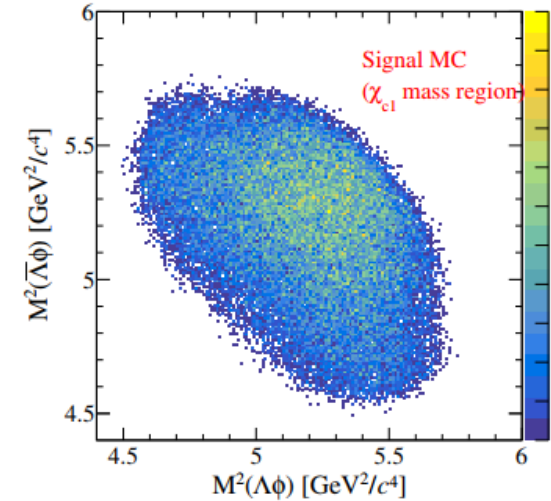
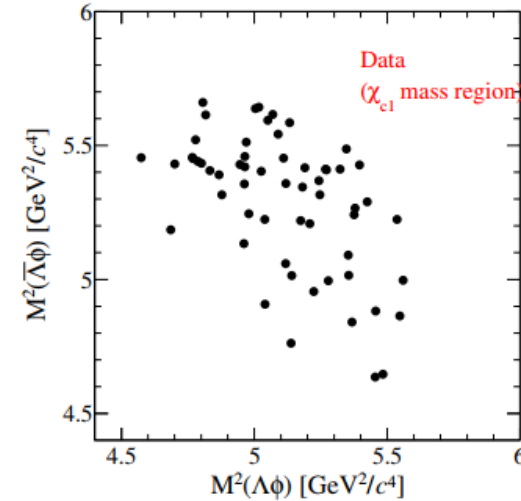
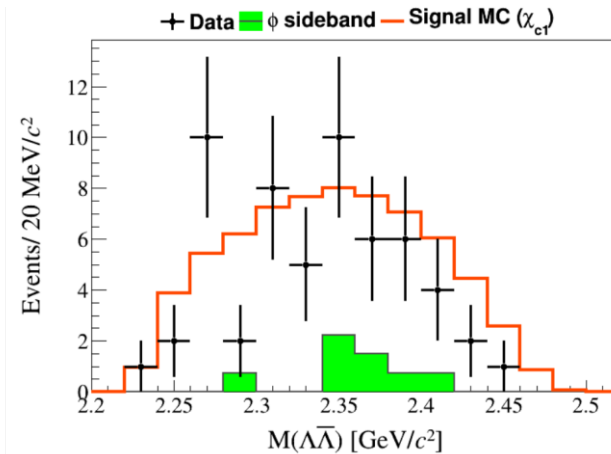
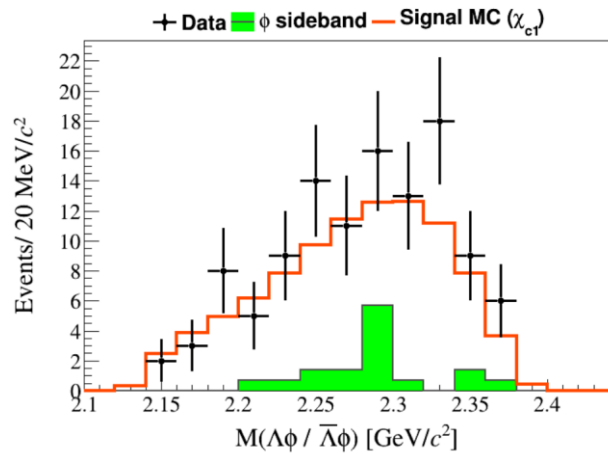


To investigate **possible background from continuum processes**, the same selection criteria are applied to a data sample of collected at $\sqrt{s} = 3.65$ GeV.
No events survived from the data at 3.65 GeV.



Dalitz Plot (I)

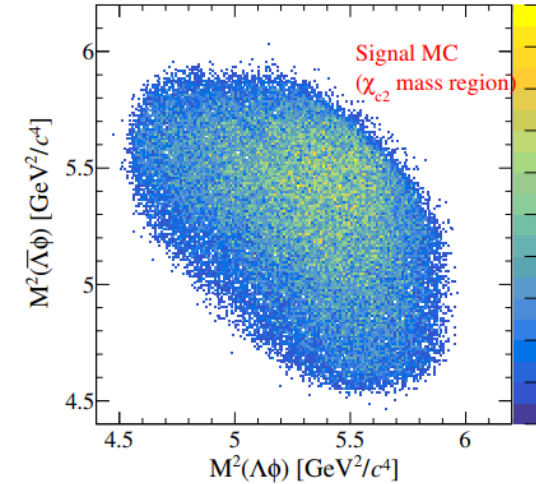
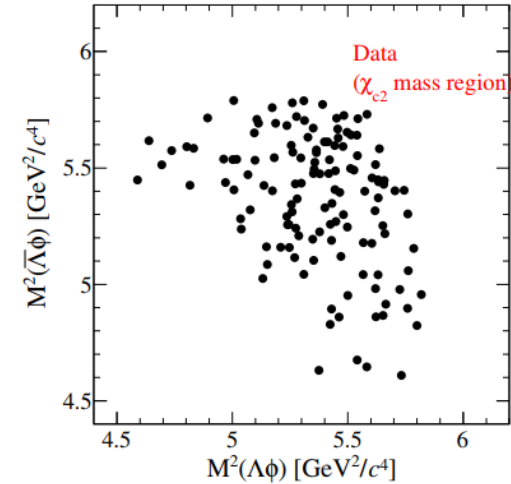
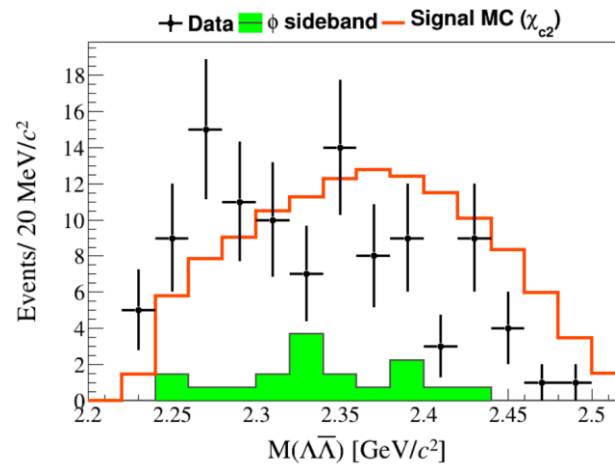
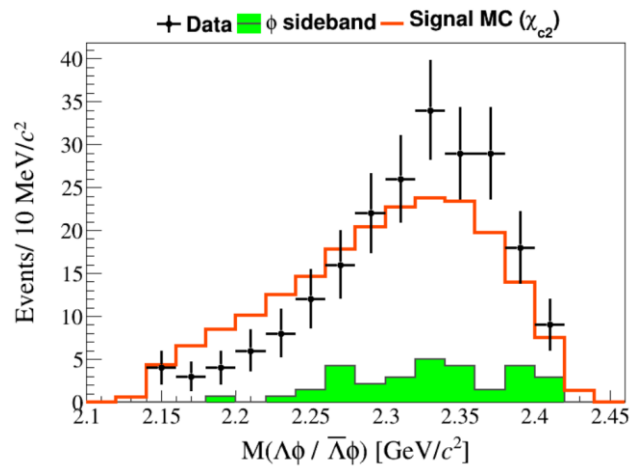
in χ_{c1} mass region



- According to the 2-D Dalitz and 1-D project plots, one is hard to draw any solid conclusion whether there are intermediate states in $M_{(\Lambda\bar{\Lambda})}$ and $M_{(\phi\Lambda)}$ based on the current statistics or not.

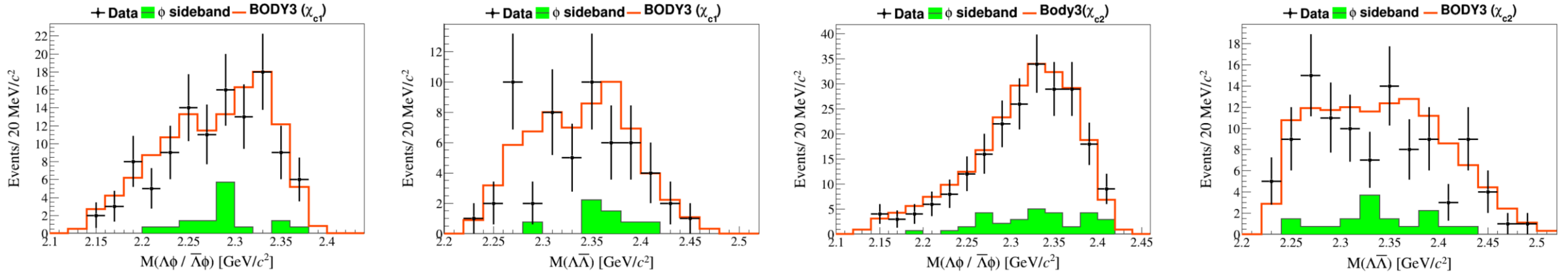
Dalitz Plot (II)

in χ_{c2} mass region



- According to the 2-D Dalitz and 1-D project plots, one is hard to draw any solid conclusion whether there are intermediate states in $M_{(\Lambda\bar{\Lambda})}$ and $M_{(\phi\Lambda)}$ based on the current statistics or not.

Detection efficiencies

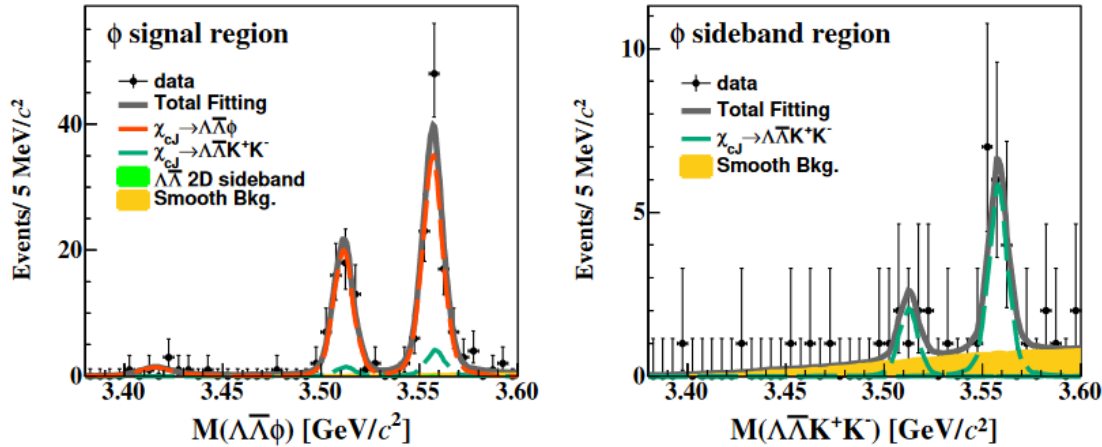


□ To determine the signal efficiencies (ϵ), the $\chi_{c1,2} \rightarrow \Lambda \bar{\Lambda} \phi$ decay channel is simulated with a modified data-driven generator BODY3, which was developed to simulate different intermediate states in data for a given three-body final state.

- The detection efficiency for $\chi_{c0,1,2} \rightarrow \Lambda \bar{\Lambda} \phi$ is estimated to be:

0.45%, 1.6% and 2.6% , respectively.

Fit to data



$$\mathcal{B}(\chi_{cJ} \rightarrow \Lambda \bar{\Lambda} \phi) = \frac{N_{\chi_{cJ}}^{\text{obs}}}{N_{\psi(3686)}^{\text{tot}} \cdot \mathcal{B}(\psi(3686) \rightarrow \gamma \chi_{cJ}) \cdot \mathcal{B}(\Lambda \rightarrow p \pi^-) \cdot \mathcal{B}(\bar{\Lambda} \rightarrow \bar{p} \pi^+) \cdot \mathcal{B}(\phi \rightarrow K^+ K^-) \cdot \epsilon_{\chi_{cJ}}}$$

- Assume that $N_{\psi(3686)}^{\text{data}} = 2.7 \text{ Billion}$

Mode	N^{obs}	$\epsilon(\%)$	$\mathcal{B}(\times 10^{-5})$	Significance(σ)
$\chi_{c0} \rightarrow \phi \Lambda \bar{\Lambda}$	7.2 ± 3.0	0.45	3.01 ± 1.25	4.7
$\chi_{c1} \rightarrow \phi \Lambda \bar{\Lambda}$	51.5 ± 7.7	1.6	6.08 ± 0.91	11.5
$\chi_{c2} \rightarrow \phi \Lambda \bar{\Lambda}$	93.7 ± 10.7	2.6	6.97 ± 0.80	14.5

- For the decay of $\chi_{cJ} \rightarrow \Lambda \bar{\Lambda} \phi$ (**ϕ signal region**), the fitting function is described as below :

$$N_{\chi_{cJ}}^{\text{obs}} \cdot \text{SigMCShape} \otimes \text{Gauss} + f_{\phi} \cdot N_{\text{bkg}}^{\phi SD} \cdot \phi - \text{SDMCShape} + N_{\text{bkg}}^{2D \sim SD} \cdot 2D - \text{SDMCShape} + N_{\text{bkg}}^{\text{flat I}} \cdot \text{BkgMCShape}$$

- The **$\phi - \text{SDMCShape}$** is the MC-simulated shape of decay $\psi(3686) \rightarrow \gamma \chi_{cJ}, \chi_{cJ} \rightarrow \Lambda \bar{\Lambda} K^+ K^-$
- The **$2D - \text{SDMCShape}$** is the the MC-simulated shape of decay $\psi(3686) \rightarrow \gamma \chi_{cJ}, \chi_{cJ} \rightarrow \phi p \pi^- \bar{p} \pi^+$
- The **BkgMCShape** is the MC-simulated shape of decay $\psi(3686) \rightarrow \gamma \Lambda \bar{\Lambda} \phi$
- $N_{\text{bkg}}^{\phi SD}$ is taken as the common parameter among the two modes.
- The scale factor f_{ϕ} between ϕ signal and sideband region is determined to be 0.71 by the integral of sideband and signal region.

- For the decay of $\chi_{cJ} \rightarrow \Lambda \bar{\Lambda} \phi$ (**ϕ sideband region**), the fitting function is described as below:

$$N_{\text{bkg}}^{\phi SD} \cdot \phi - \text{SDMCShape} + N_{\text{bkg}}^{\text{flat II}} \cdot \text{BkgMCShape}$$

Determining the statistical significance of χ_{c0}

- Assuming that the numbers of total events (n) in χ_{c0} signal region, $n = s + b$, s and b denote signal and background, respectively. We recalculated the significance of $\chi_{c0} \rightarrow \Lambda \bar{\Lambda} \phi$ according to the p-value equation as,

$$P(n_{\text{obs}}) = P(n | > n_{\text{obs}} | H_0) = \sum_{n=n_{\text{obs}}}^{\infty} \frac{b^n}{n!} e^{-b} = 1 - \sum_{n=0}^{n_{\text{obs}}-1} \frac{b^n}{n!} e^{-b}$$

If taking 2σ width as the signal region, we have $n = 7$, $b = 0.6$, and $s = [n - b] \approx 6$. Suppose $s = 0$, P-value = 3.29×10^{-6} . The statistical significance is determined to be 4.6σ according to the corresponding P value.

- Therefore, the statistical significance of $\chi_{c0} \rightarrow \Lambda \bar{\Lambda} \phi$ is not less than 4.6σ .

Systematic uncertainty [I]

I. Total number of $\psi(3686)^{[1]}$

II. Tracking for kaon and photon reconstruction efficiencies*

The uncertainty on the tracking efficiency and photon with the control samples $J/\psi \rightarrow K_S^0 K^\pm \pi^\mp$ and $J/\psi \rightarrow \pi^+ \pi^- \pi^0$, respectively, and are determined to be 1.0% for each charged kaon and per photon.

III. PID for Kaon*

The kaon identification efficiency have been studied by the BESIII Collaboration. The differences between data and Monte Carlo samples are estimated to be within kaon.

IV. Mass window: The main Background comes from decay

$\chi_{cJ} \rightarrow \Omega^- \bar{\Omega}^+$, ϕ mass window and $\Lambda(\bar{\Lambda})$ mass window.

- The systematic uncertainty on the above mass window is obtained by changing the interval comparison of the mass window.

V. Scale factor f_ϕ

The systematic uncertainty on scale factor f_ϕ is obtained by changing the sideband region (changing the signal region by $\pm 1\sigma$).

VI. Kinematic fit : Two control samples are employed to study the systematic error due to 4-C kinematic fit, the are $\psi(3686) \rightarrow \pi^+ \pi^- J/\psi$, $J/\psi \rightarrow \Lambda \bar{\Lambda}$ and $\psi(3686) \rightarrow \eta J/\psi$, $J/\psi \rightarrow \pi^+ \pi^- \Lambda \bar{\Lambda}$.

- The signal events is extracted once again after imposing the 4-C kinematic fit on the candidate charged and neutral track. We define the efficiency of 4-C kinematic fit systematic uncertainty as below:

$$\epsilon_{4C} = \frac{N_{obs}(with-4Cfit)}{N_{obs}(without-4Cfit)}$$

The difference between data and inclusive MC is found to be systematic uncertainty. And, the largest one is found to be **1.2%**.

Systematic uncertainty [II]

VII. $\Lambda(\bar{\Lambda})$ reconstruction: The systematic uncertainty of $\Lambda(\bar{\Lambda})$ reconstruction is studied using the control sample of $J/\psi \rightarrow pK^-\bar{\Sigma}^0 (\rightarrow \gamma\bar{\Lambda}) + c.c..$

- For reconstruction efficiency of $\Lambda(\bar{\Lambda})$ in the process $J/\psi \rightarrow pK^-\Sigma^0 (\rightarrow \gamma\Lambda)$, we tag $\bar{p}K^+(pK^-\gamma)$ candidates, and **fit the recoil mass of $\bar{p}K^+(pK^-\gamma)$** to estimate the number of $\Lambda(\bar{\Lambda})$ **yield**.

The combined efficiency of tracking and reconstruction for Λ and $\bar{\Lambda}$ have been given by using the control sample of $J/\psi \rightarrow pK^-\bar{\Sigma}^0 (\rightarrow \gamma\bar{\Lambda})$ to be **1.8%** and **1.5%**, respectively.

VIII. Systematic uncertainty on fit

- **Signal Shape:** The uncertainty caused by signal function is estimated by removing the Gaussian convolution in MC-simulated shape.
- **Background shape:** The uncertainties due to the background shape is estimated by replacing the nominal parameterized MC shape, which is obtained by the MC sample of $\psi(3683) \rightarrow \gamma\Lambda\bar{\Lambda}\phi$, with second order polynomial.
- **Fitting range:** By changing the fitting range, the one with greatest difference from the original result is taken as the systematic uncertainty.

IX. MC generator

- To study the systematic uncertainty in the modified MC generator, we varying $\pm 1\sigma$ for the level of background in the input Dalitz plot, where the σ denotes the statistical uncertainty of the background which determined from the fit result. The largest change to the nominal detection efficiency is taken as the systematic uncertainty, which the uncertainty values of $\chi_{c1,2}$ are determined to be 2.5% and 0.4%, respectively.

IX. Branching fraction quoted

- The uncertainties to the quoted decay branching fraction of the intermediate particles are extracted from the PDG.

Systematic uncertainty [III]

Mode:	$\chi_{c0} \rightarrow \Lambda \bar{\Lambda} \phi$	$\chi_{c1} \rightarrow \Lambda \bar{\Lambda} \phi$	$\chi_{c2} \rightarrow \Lambda \bar{\Lambda} \phi$
Tracking for Kaon	2.0%	2.0%	2.0%
Kaon PID	2.0%	2.0%	2.0%
Photon detection	1.0%	1.0%	1.0%
Mass window	2.1%	2.0%	2.1%
Scale factor f_ϕ	0.3%	0.2%	0.3%
Kinematic fit	1.3%	1.3%	1.3%
Λ reconstruction	1.8%	1.8%	1.8%
$\bar{\Lambda}$ reconstruction	1.5%	1.5%	1.5%
Signal range	1.1%	0.4%	0.3%
Background shape	0.4%	1.8%	Negligible
Fitting range	1.8%	1.1%	1.0%
MC generator	-	2.5%	0.4%
Branching fraction quoted	2.5%	2.9%	2.6%
The total number of $\psi(3686)$	1.0%	1.0%	1.0%
Total	5.7%	6.4%	5.4%

Summary & Next to do

- ✓ Signal of $\chi_{c1,2} \rightarrow \Lambda \bar{\Lambda} \phi$ **are observed** with significance of 11.5σ and 14.5σ , respectively.
 - ✓ The evidence of $\chi_{c0} \rightarrow \Lambda \bar{\Lambda} \phi$ is observed with significance **of 4.6σ** above.
 - ✓ No obvious structure found in the $\Lambda \phi$ and $\Lambda \bar{\Lambda}$ system .
 - ✓ Estimate the systematic uncertainty.
-

Next to do

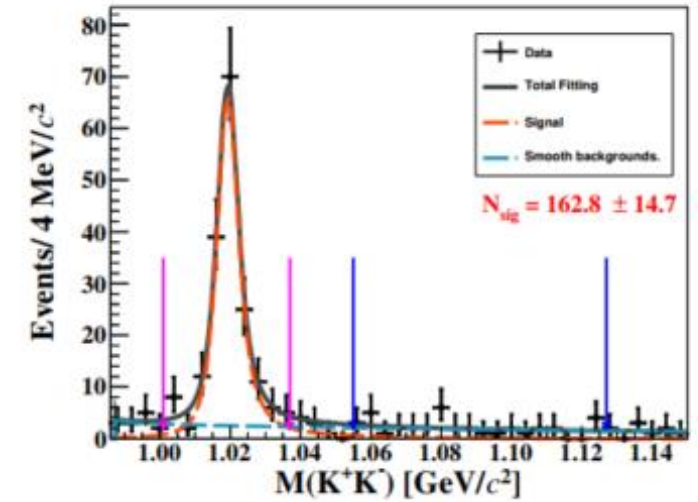
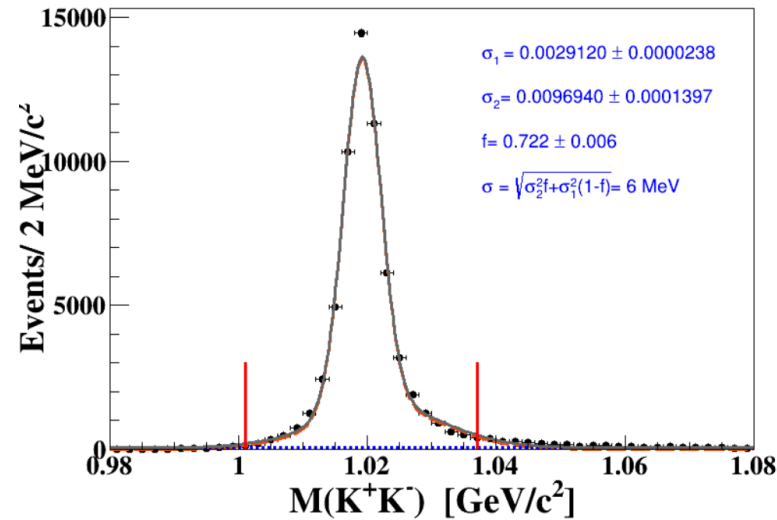
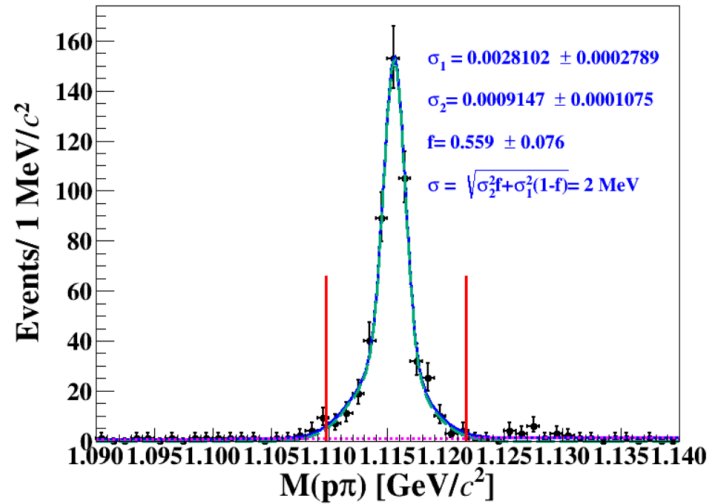
- Preparing for the P&S meeting

Thank You! 😊

Thank You!

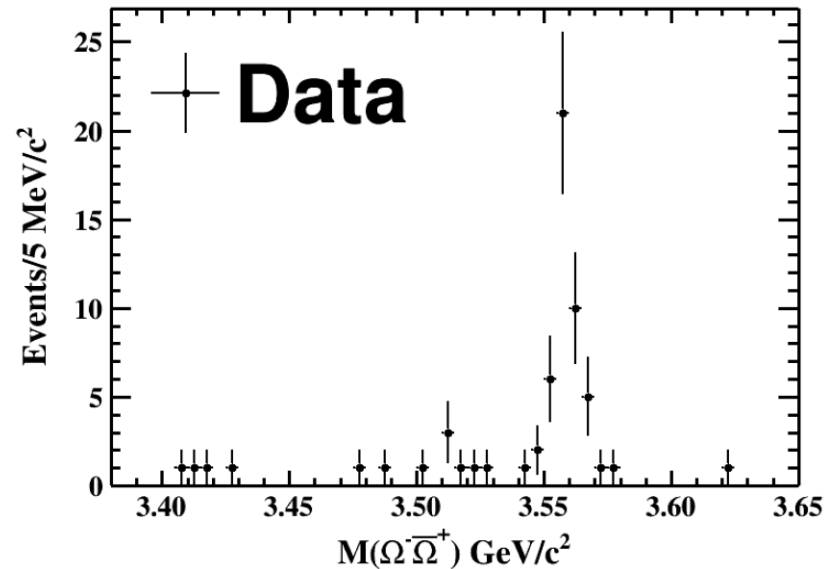
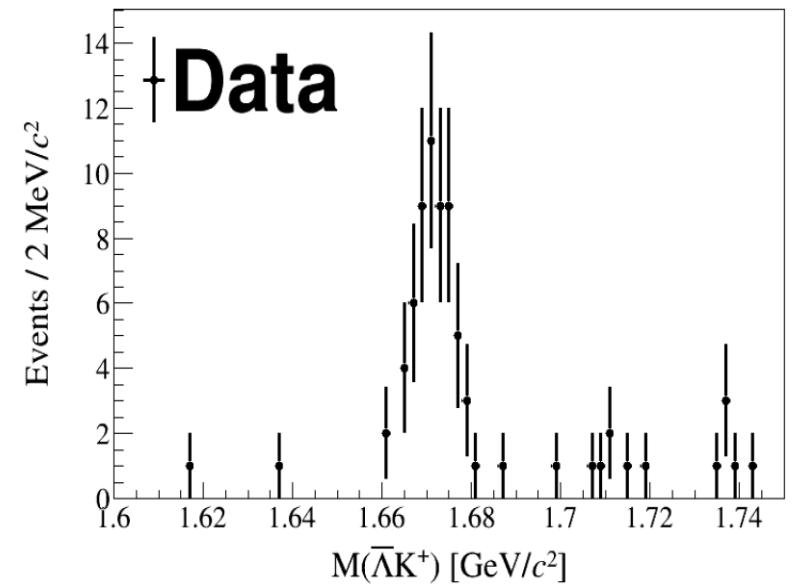
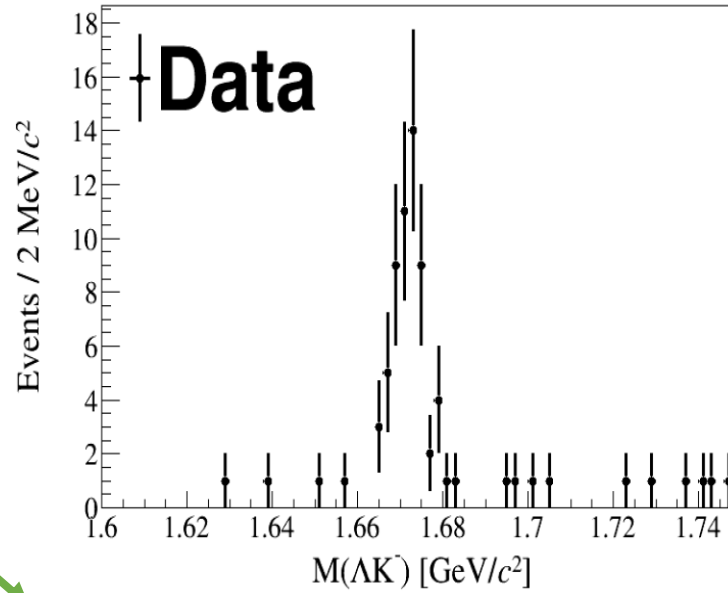
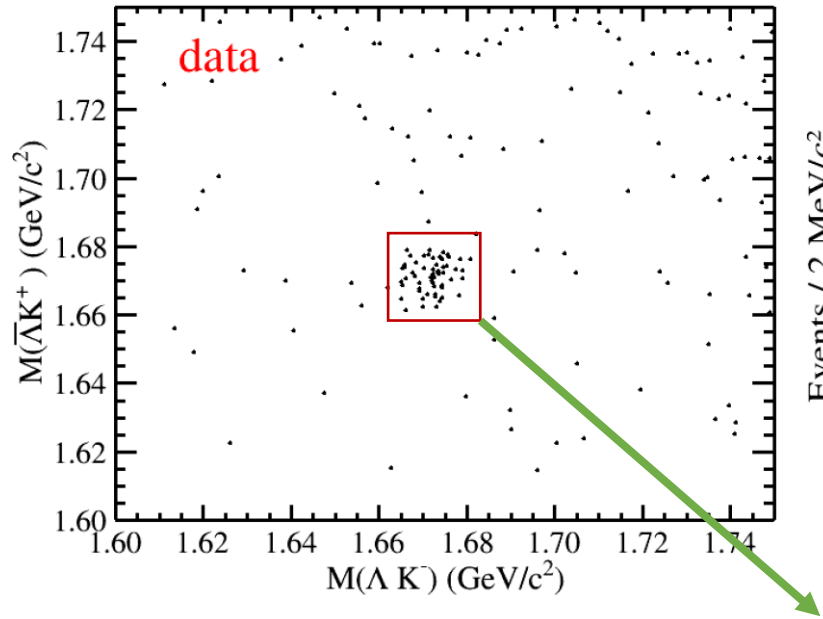
:)

Back up

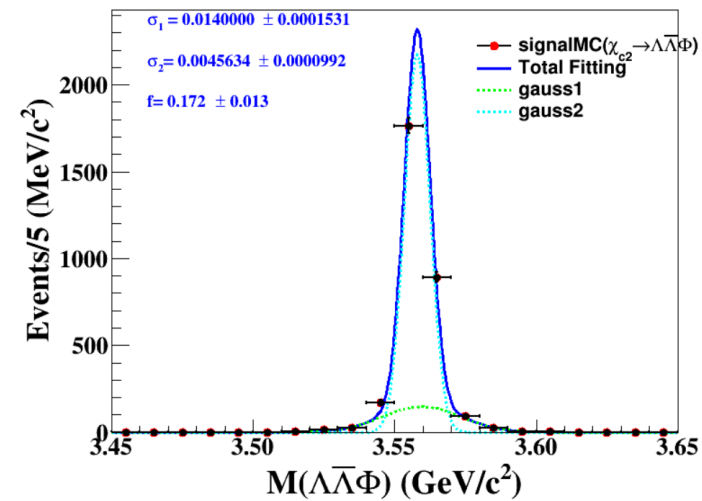
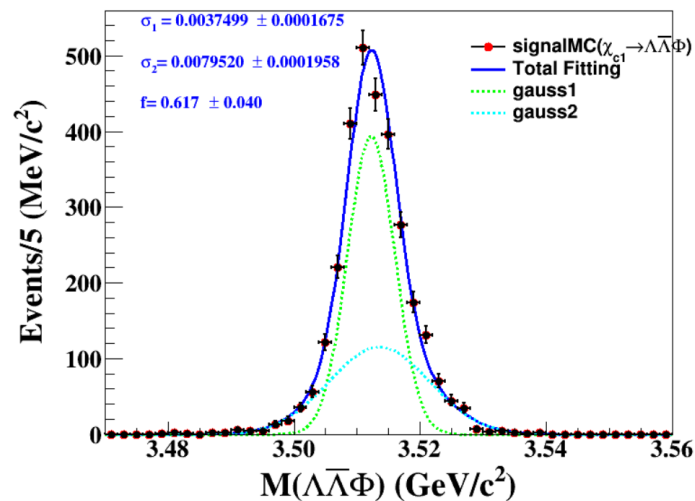
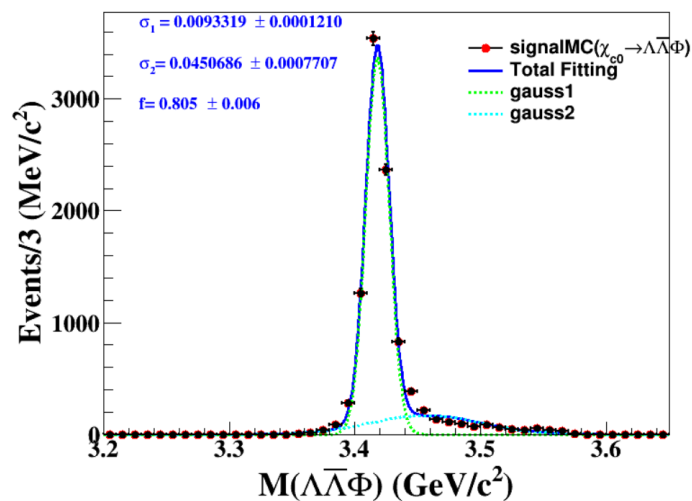


- We fit the mass spectrum of $p\pi$, $\sigma_{p\pi} = 2\text{MeV}$.
- We fit the mass spectrum of K^+K^- , $\sigma = 6\text{MeV}$. And a sideband region is selected.
 $1.055 < M(K^+K^-)_{\text{sideband}} < 1.091 \text{ GeV}/c^2$
- The scale factor f_ϕ between ϕ signal and sideband region is determined to be 0.71 by the integral of sideband and signal region.

$$\chi_{cJ} \rightarrow \Omega^- \bar{\Omega}^+$$



Back up



Systematic uncertainty of Mass window

Mode	$\chi_{c0} \rightarrow \Lambda \bar{\Lambda} \phi$	$\chi_{c1} \rightarrow \Lambda \bar{\Lambda} \phi$	$\chi_{c2} \rightarrow \Lambda \bar{\Lambda} \phi$
ϕ mass window	6.1%	1.5%	1.5%
$\Lambda \bar{\Lambda}$ 2-D mass window	2.9%	1.3%	1.1%
$\Omega^- \bar{\Omega}^+$ 2-D mass window	1.7%	0.4%	1.0%
Fit	7.0%	2.0%	2.1%

Systematic uncertainty of 4-C Kinematic fit[1]

Event selection of control sample: $\psi \rightarrow \pi^+ \pi^- J/\psi$, $J/\psi \rightarrow \Lambda \bar{\Lambda}$

■ Charge track

- With the same selection criteria as $\psi(3686) \rightarrow \gamma \chi_{cJ} \rightarrow \gamma \Lambda \bar{\Lambda}$
- $N_{\text{positive}} \geq 3, N_{\text{negative}} \geq 3$

■ $\Lambda (\bar{\Lambda})$ reconstruction

Looping over all the combination of positive and negative charged tracks pairs.

We require two virtual particle, Λ and $\bar{\Lambda}$ can be reconstructed in this combinations. Then ,the minimum mass deviation is combined of $\Lambda \bar{\Lambda}$ to selected them.

$$\Delta_{\min} = (M_{p\pi^-} - m_{\Lambda})^2 + (M_{\bar{p}\pi^+} - m_{\bar{\Lambda}})^2 \Rightarrow \Lambda_{\min}, \bar{\Lambda}_{\min}$$

■ π^+ and π^- (not from Λ or $\bar{\Lambda}$ decay) selection

- the charged track not belonging to any of $\Lambda(\bar{\Lambda})$ candidates
- $|V_z| < 10, |V_{xy}| < 1$

Table 8: Decay trees and their respective final states.

No.	Decay Chain	Final states	nEvt
1	$\psi(3686) \rightarrow \pi^+ \pi^- J/\psi, J/\psi \rightarrow \Lambda \bar{\Lambda}$	$\pi^+ \pi^+ \pi^- \pi^- p \bar{p}$	128809
2	$\psi(3686) \rightarrow \Lambda \bar{\Lambda} \pi^+ \pi^-$	$\pi^+ \pi^+ \pi^- \pi^- p \bar{p} \gamma \gamma$	1490
3	$\psi(3686) \rightarrow \pi^+ \pi^- J/\psi, J/\psi \rightarrow \Lambda \bar{\Lambda} \gamma$	$\pi^+ \pi^+ \pi^- \pi^- p \bar{p} \gamma$	849
4

Systematic uncertainty of 4-C Kinematic fit[2]

Event selection of control sample: $\psi \rightarrow \eta J/\psi, J/\psi \rightarrow \Lambda \bar{\Lambda} \pi^+ \pi^-$

■ Charge track

- With the same selection criteria as $\psi(3686) \rightarrow \gamma \chi_{cJ} \rightarrow \gamma \Lambda \bar{\Lambda}$
- $N_{\text{positive}} \geq 3, N_{\text{negative}} \geq 3$

■ Good photon

- $N_{\gamma} \geq 2$

■ $\Lambda (\bar{\Lambda})$ reconstruction

Looping over all the combination of positive and negative charged tracks pairs. We require two virtual particle, Λ and $\bar{\Lambda}$ can be reconstructed in this combinations. Then ,the minimum mass deviation is combined of $\Lambda \bar{\Lambda}$ to selected them.

$$\Delta_{\min} = (M_{p\pi^-} - m_{\Lambda})^2 + (M_{p\pi^+} - m_{\bar{\Lambda}})^2 \Rightarrow \Lambda_{\min}, \bar{\Lambda}_{\min}$$

■ η reconstruction

- A 1C-kinematic fit is performed on the selected photon pairs by constraining their invariant mass to the η mass.

■ π^+ and π^- (not from Λ or $\bar{\Lambda}$ decay) selection

- the charged track not belonging to any of $\Lambda(\bar{\Lambda})$ candidates
- $|V_z| < 10, |V_{xy}| < 1$

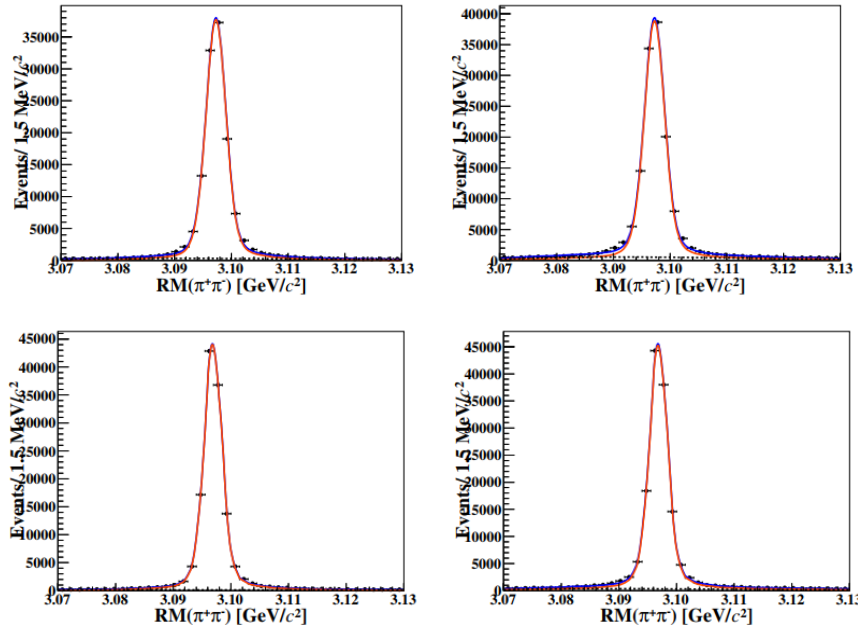
Table 10: Decay trees and their respective final states.

No.	Decay Chain	Final states	nEvt
1	$\psi(3686) \rightarrow \eta J/\psi, J/\psi \rightarrow \Lambda \bar{\Lambda} \pi^+ \pi^-$	$\pi^+ \pi^+ \pi^- \pi^- p \bar{p} \gamma \gamma$	4827
2	$\psi(3686) \rightarrow \pi^0 \pi^0 J/\psi, J/\psi \rightarrow \Lambda \bar{\Lambda} \pi^+ \pi^-$	$\pi^+ \pi^+ \pi^- \pi^- p \bar{p} \gamma \gamma$	1466
3	$\psi(3686) \rightarrow \gamma \chi_{cJ}, \chi_{cJ} \rightarrow \gamma J/\psi, J/\psi \rightarrow \Lambda \bar{\Lambda} \pi^+ \pi^-$	$\pi^+ \pi^+ \pi^- \pi^- p \bar{p} \gamma \gamma$	101
4

Systematic uncertainty of 4-C Kinematic fit[3]

control sample :

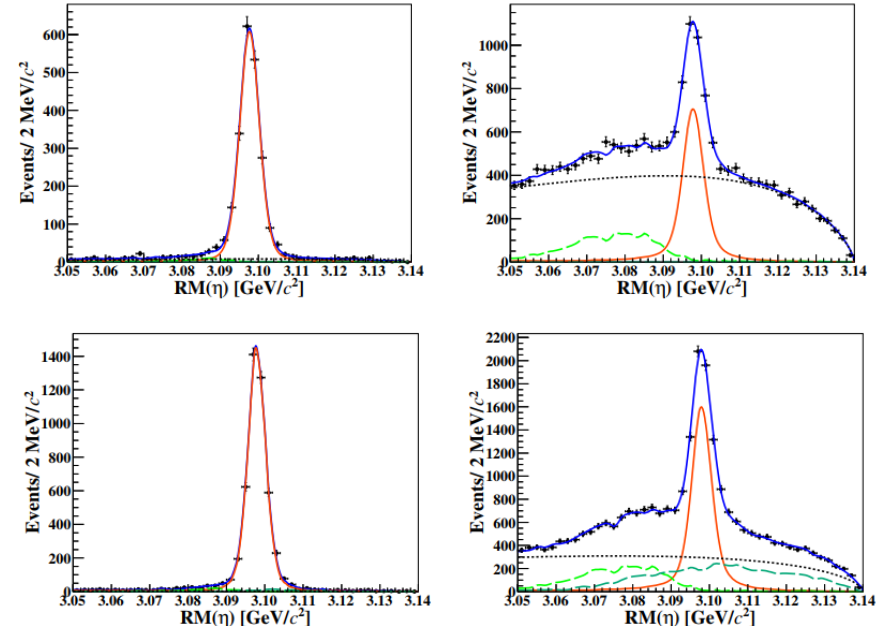
$$\psi \rightarrow \pi^+ \pi^- J/\psi, J/\psi \rightarrow \Lambda \bar{\Lambda}$$



	Data(fit)	Inc. MC(fit)
With K.F. ($\chi^2_{4c} < 60$)	120360.4 ± 373.5	124865.1 ± 371.7
Without K.F.	136699.0 ± 423.2	141341.4 ± 420.4
Efficiency($\epsilon\%$)	88.1	88.3
$\Delta(\%)$	0.2	

control sample:

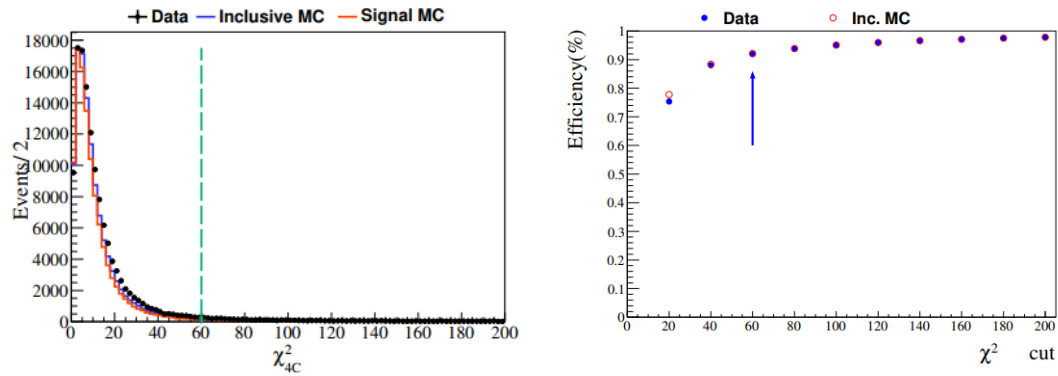
$$\psi \rightarrow \eta J/\psi, J/\psi \rightarrow \Lambda \bar{\Lambda} \pi^+ \pi^-$$



	Data(fit)	Inc. MC(fit)
With K.F. ($\chi^2_{4c} < 60$)	2158.5 ± 53.4	4619.3 ± 75.9
Without K.F.	2960.9 ± 106.3	6413.6 ± 134.5
Efficiency($\epsilon\%$)	72.0	72.9
$\Delta(\%)$	1.2	

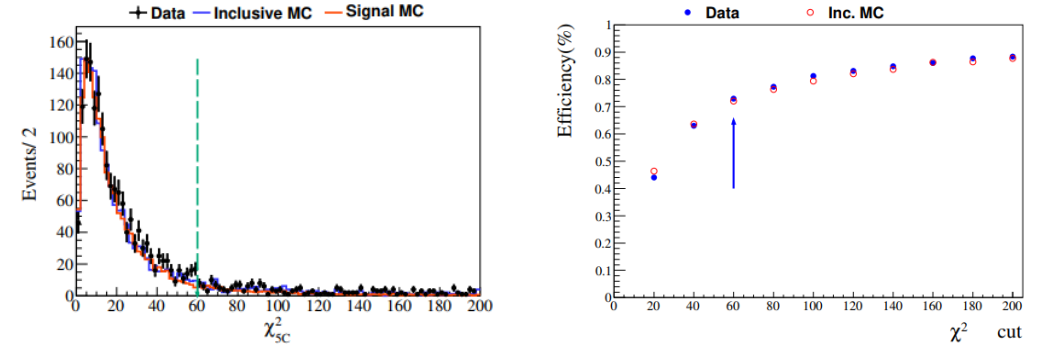
Systematic uncertainty of 4-C Kinematic fit[3]

control sample :
 $\psi \rightarrow \pi^+ \pi^- J/\psi, J/\psi \rightarrow \Lambda \bar{\Lambda}$



$$\chi^2 < 60, \epsilon_{4C} = 0.2\%$$

control sample:
 $\psi \rightarrow \eta J/\psi, J/\psi \rightarrow \Lambda \bar{\Lambda} \pi^+ \pi^-$



$$\chi^2 < 60, \epsilon_{5C} = 1.2\%$$

Systematic uncertainty of combined tracking and recons.-efficiency of $\bar{\Lambda}$ [II]

control sample II: $J/\psi \rightarrow pK^- \bar{\Sigma}^0$, $\bar{\Sigma}^0 \rightarrow \gamma \bar{\Lambda}$ (for *Partial reconstruction*)

■ Charge track

- $|\cos\theta| < 0.93$
- $N_{\text{positive}} \geq 1, N_{\text{negative}} \geq 1$
- No vertex constraint

■ Good photon

- regular conditions
- $N_\gamma \geq 1$
- Requires the momentum of the photon $< 140\text{MeV}$

■ PID

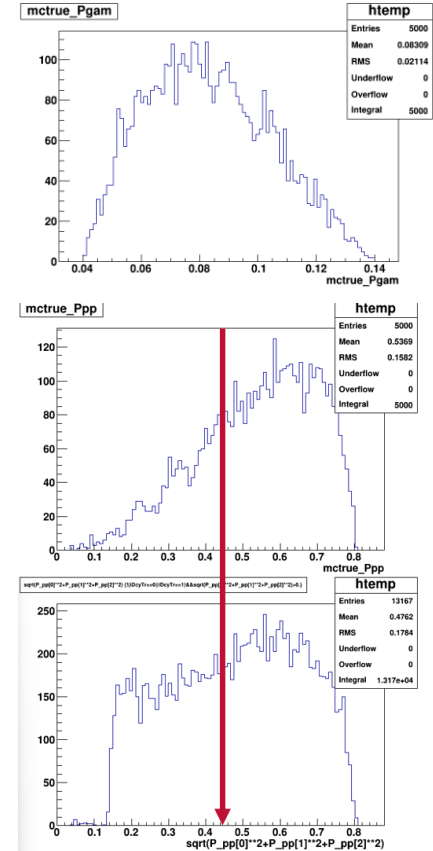
- $N(p) > 1, N(K^-) > 1$
- $|V_z| < 3\text{cm}, |V_{xy}| < 0.2\text{cm}$

■ $\text{RM}(pK^- \gamma)$

- By minimizing the mass deviation(Δ) of $\text{RM}(pK^- \gamma)$:

$$\Delta_{\min} = |\sqrt{(RM_{(pK^- \gamma)} - m_\Lambda)^2}|$$

- To suppress the background, $RM_{(pK^-)} \in (1.185, 1.205) \text{ GeV}/c^2$ and $P(p) > 0.45 \text{ GeV}$ are required.



Systematic uncertainty of combined tracking and recons.-efficiency of $\bar{\Lambda}$ [II]

control sample II: $J/\psi \rightarrow pK^-\bar{\Sigma}^0, \bar{\Sigma}^0 \rightarrow \gamma\bar{\Lambda}$ (for *Full reconstruction*)

■ Charge track

- $|\cos\theta| < 0.93$
- $N_{\text{positive}} \geq 2, N_{\text{negative}} \geq 2$
- No vertex constraint

■ Good photon

- Regular conditions
- $N_\gamma \geq 1$
- Requires the momentum of the photon $< 140\text{MeV}$

■ $\bar{\Lambda}$ reconstruction

- With the same selection criteria as $\psi(3686) \rightarrow \gamma\chi_{cJ} \rightarrow \gamma\Lambda\bar{\Lambda}$

■ PID

- The charged track not belonging to any of $\bar{\Lambda}$ candidates.
- $|V_z| < 3\text{cm}, |V_{xy}| < 0.2\text{cm}$
- $N(p) > 1, N(K^-) > 1$

■ $\text{RM}(pK^-\gamma)$

- By minimizing the mass deviation(Δ) of $\text{RM}(pK^-\gamma)$:

$$\Delta_{\min} = |\sqrt{(RM_{(pK^-\gamma)} - m_\Lambda)^2}|$$

- To suppress the background, $RM_{(pK^-)} \in (1.185, 1.205) \text{ GeV}/c^2$ and $P(p) > 0.45 \text{ GeV}$ are required.

Systematic uncertainty of combined tracking and recons.-efficiency of $\bar{\Lambda}$ [II]

Peaking
background

Signal
channel

Table 1: Decay trees and their respective final states.

rowNo	decay tree	decay final state	iDcyTr	nEtr	nCEtr
1	$J/\psi \rightarrow K^- p \bar{\Sigma}^0, \bar{\Sigma}^0 \rightarrow \bar{\Lambda} \gamma, \bar{\Lambda} \rightarrow \pi^+ \bar{p}$	$\pi^+ K^- p \bar{p} \gamma$	0	27997	27997
2	$J/\psi \rightarrow K^- p \bar{\Sigma}^0, \bar{\Sigma}^0 \rightarrow \bar{\Lambda} \gamma, \bar{\Lambda} \rightarrow \pi^0 \bar{n}$	$\pi^0 K^- \bar{n} p \gamma$	1	21689	49686
3	$J/\psi \rightarrow K^- p \bar{\Lambda}, \bar{\Lambda} \rightarrow \pi^+ \bar{p}$	$\pi^+ K^- p \bar{p}$	15	2323	52009
4	$J/\psi \rightarrow \pi^+ \pi^- p \bar{p}$	$\pi^+ \pi^- p \bar{p}$	2	949	52958
5	$J/\psi \rightarrow \pi^+ p \bar{\Delta}^{++}, \bar{\Delta}^{++} \rightarrow \pi^- \bar{p}$	$\pi^+ \pi^- p \bar{p}$	21	425	53383
6	$J/\psi \rightarrow \pi^- \bar{p} \bar{\Delta}^{++}, \bar{\Delta}^{++} \rightarrow \pi^+ p$	$\pi^+ \pi^- p \bar{p}$	28	272	53655
7	$J/\psi \rightarrow \Delta^{++} \bar{\Delta}^{++}, \bar{\Delta}^{++} \rightarrow \pi^+ p, \bar{\Delta}^{++} \rightarrow \pi^- \bar{p}$	$\pi^+ \pi^- p \bar{p}$	20	261	53916
8	$J/\psi \rightarrow \pi^0 \pi^+ \pi^- p \bar{p}$	$\pi^0 \pi^+ \pi^- p \bar{p}$	19	227	54143
9	$J/\psi \rightarrow K^- p \bar{\Sigma}^0, \bar{\Sigma}^0 \rightarrow \bar{\Lambda} \gamma, \bar{\Lambda} \rightarrow \pi^0 \bar{n}, \pi^0 \rightarrow e^+ e^- \gamma^F$	$e^+ e^- K^- \bar{n} p \gamma^F \gamma$	41	206	54349
10	$J/\psi \rightarrow \pi^0 \Delta^{++} \bar{\Delta}^{++}, \bar{\Delta}^{++} \rightarrow \pi^+ p, \bar{\Delta}^{++} \rightarrow \pi^- \bar{p}$	$\pi^0 \pi^+ \pi^- p \bar{p}$	40	203	54552
11	$J/\psi \rightarrow \omega p \bar{p}, \omega \rightarrow \pi^0 \pi^+ \pi^-$	$\pi^0 \pi^+ \pi^- p \bar{p}$	11	169	54721
12	$J/\psi \rightarrow \pi^- \bar{\Delta}^+ \Delta^{++}, \bar{\Delta}^+ \rightarrow \pi^0 \bar{p}, \Delta^{++} \rightarrow \pi^+ p$	$\pi^0 \pi^+ \pi^- p \bar{p}$	45	135	54856
13	$J/\psi \rightarrow \pi^0 \Delta^+ \bar{\Delta}^+, \bar{\Delta}^+ \rightarrow \pi^0 p, \bar{\Delta}^+ \rightarrow \pi^0 \bar{p}$	$\pi^0 \pi^0 \pi^0 p \bar{p}$	39	126	54982
14	$J/\psi \rightarrow K^- p \bar{\Sigma}^{*0}, \bar{\Sigma}^{*0} \rightarrow \pi^0 \bar{\Lambda}, \bar{\Lambda} \rightarrow \pi^+ \bar{p}$	$\pi^0 \pi^+ K^- p \bar{p}$	67	124	55106
15	$J/\psi \rightarrow \pi^0 \pi^+ \pi^- K^+ K^-$	$\pi^0 \pi^+ \pi^- K^+ K^-$	86	118	55224
16	$J/\psi \rightarrow \pi^- \bar{\Delta}^0 p, \bar{\Delta}^0 \rightarrow \pi^+ \bar{p}$	$\pi^+ \pi^- p \bar{p}$	14	116	55340
17	$J/\psi \rightarrow \pi^- \bar{K}^* K^{*+}, \bar{K}^* \rightarrow \pi^+ K^-, K^{*+} \rightarrow \pi^+ K^0, K^0 \rightarrow K_L^0$	$K_L^0 \pi^+ \pi^+ \pi^- K^-$	10	116	55456
18	$J/\psi \rightarrow K^- p \bar{\Sigma}^0, \bar{\Sigma}^0 \rightarrow \bar{\Lambda} \gamma, \bar{\Lambda} \rightarrow \bar{n} \gamma$	$K^- \bar{n} p \gamma \gamma$	83	98	55554
19	$J/\psi \rightarrow \eta e \gamma, \eta e \rightarrow K^- p \bar{\Lambda}, \bar{\Lambda} \rightarrow \pi^+ \bar{p}$	$\pi^+ K^- p \bar{p} \gamma$	93	95	55649
20	$J/\psi \rightarrow \pi^0 \pi^- \bar{n} p$	$\pi^0 \pi^- \bar{n} p$	35	94	55743
21	$J/\psi \rightarrow \rho^- \bar{K}^* K^{*+}, \rho^- \rightarrow \pi^0 \pi^-, \bar{K}^* \rightarrow \pi^+ K^-, K^{*+} \rightarrow \pi^+ K^0, K^0 \rightarrow K_L^0$	$\pi^0 K_L^0 \pi^+ \pi^+ \pi^- K^-$	43	91	55834
22	$J/\psi \rightarrow \pi^- \bar{\Delta}^0 \Delta^+, \bar{\Delta}^0 \rightarrow \pi^0 \bar{n}, \Delta^+ \rightarrow \pi^0 p$	$\pi^0 \pi^0 \pi^- \bar{n} p$	17	66	55900
23	$J/\psi \rightarrow \pi^0 \pi^0 p \bar{p}$	$\pi^0 \pi^0 p \bar{p}$	146	66	55966

Table 1: Decay trees and their respective final states.

rowNo	decay tree	decay final state	iDcyTr	nEtr	nCEtr
1	$J/\psi \rightarrow K^- p \bar{\Sigma}^0, \bar{\Sigma}^0 \rightarrow \bar{\Lambda} \gamma, \bar{\Lambda} \rightarrow \pi^+ \bar{p}$	$\pi^+ K^- p \bar{p} \gamma$	0	21201	21201
2	$J/\psi \rightarrow K^- p \bar{\Sigma}^0, \bar{\Sigma}^0 \rightarrow \bar{\Lambda} \gamma, \bar{\Lambda} \rightarrow \pi^0 \bar{n}$	$\pi^0 K^- \bar{n} p \gamma$	14	440	21641
3	$J/\psi \rightarrow \pi^+ \pi^- p \bar{p}$	$\pi^+ \pi^- p \bar{p}$	3	313	21954
4	$J/\psi \rightarrow \pi^0 \Delta^{++} \bar{\Delta}^{++}, \bar{\Delta}^{++} \rightarrow \pi^+ p, \bar{\Delta}^{++} \rightarrow \pi^- \bar{p}$	$\pi^0 \pi^+ \pi^- p \bar{p}$	2	271	22225
5	$J/\psi \rightarrow \pi^0 \pi^+ \pi^- p \bar{p}$	$\pi^0 \pi^+ \pi^- p \bar{p}$	6	230	22455
6	$J/\psi \rightarrow \omega p \bar{p}, \omega \rightarrow \pi^0 \pi^+ \pi^-$	$\pi^0 \pi^+ \pi^- p \bar{p}$	17	199	22654
7	$J/\psi \rightarrow \pi^+ p \bar{\Delta}^{++}, \bar{\Delta}^{++} \rightarrow \pi^- \bar{p}$	$\pi^+ \pi^- p \bar{p}$	21	166	22820
8	$J/\psi \rightarrow \Delta^{++} \bar{\Delta}^{++}, \bar{\Delta}^{++} \rightarrow \pi^+ p, \bar{\Delta}^{++} \rightarrow \pi^- \bar{p}$	$\pi^+ \pi^- p \bar{p}$	62	133	22953
9	$J/\psi \rightarrow \pi^- \bar{p} \bar{\Delta}^{++}, \bar{\Delta}^{++} \rightarrow \pi^+ p$	$\pi^+ \pi^- p \bar{p}$	63	127	23080
10	$J/\psi \rightarrow \pi^- \bar{\Delta}^+ \Delta^{++}, \bar{\Delta}^+ \rightarrow \pi^0 \bar{p}, \Delta^{++} \rightarrow \pi^+ p$	$\pi^0 \pi^+ \pi^- p \bar{p}$	31	104	23184
11	$J/\psi \rightarrow \rho^- \bar{K}^* K^{*+}, \rho^- \rightarrow \pi^0 \pi^-, \bar{K}^* \rightarrow \pi^+ K^-, K^{*+} \rightarrow \pi^+ K^0, K^0 \rightarrow K_L^0$	$\pi^0 K_L^0 \pi^+ \pi^+ \pi^- K^-$	33	95	23279
12	$J/\psi \rightarrow \pi^+ \pi^- K^* \bar{K}^*, K^* \rightarrow \pi^- K^+, \bar{K}^* \rightarrow \pi^+ K^-$	$\pi^+ \pi^+ \pi^- \pi^- K^+ K^-$	50	87	23366
13	$J/\psi \rightarrow \rho^- \bar{K}^* K^{*+}, \rho^- \rightarrow \pi^0 \pi^-, \bar{K}^* \rightarrow \pi^+ K^-, K^{*+} \rightarrow \pi^+ K^0, K^0 \rightarrow K_S^0$	$\pi^0 \pi^+ \pi^+ \pi^- \pi^- K^+ K^-$	26	76	23442
14	$J/\psi \rightarrow \pi^+ \Delta^+ \bar{\Delta}^{++}, \bar{\Delta}^+ \rightarrow \pi^0 p, \bar{\Delta}^{++} \rightarrow \pi^- \bar{p}$	$\pi^0 \pi^+ \pi^- p \bar{p}$	35	73	23515
15	$J/\psi \rightarrow \pi^+ \pi^- K^{*+} K^{*-}, K^{*+} \rightarrow \pi^+ K^0, K^{*-} \rightarrow \pi^0 K^-, K^0 \rightarrow K_L^0$	$\pi^0 K_L^0 \pi^+ \pi^+ \pi^- K^-$	27	69	23584
16	$J/\psi \rightarrow \pi^- \bar{K}^* K^{*+}, \bar{K}^* \rightarrow \pi^+ K^-, K^{*+} \rightarrow \pi^+ K^0, K^0 \rightarrow K_S^0, K_S^0 \rightarrow \pi^+ \pi^-$	$\pi^+ \pi^+ \pi^+ \pi^- \pi^- K^-$	49	63	23647
17	$J/\psi \rightarrow \pi^0 \pi^+ \pi^- K^+ K^-$	$\pi^0 \pi^+ \pi^- K^+ K^-$	39	63	23710
18	$J/\psi \rightarrow \pi^0 \pi^- \bar{K}^* K^{*+}, \bar{K}^* \rightarrow \pi^+ K^-, K^{*+} \rightarrow \pi^+ K^0, K^0 \rightarrow K_L^0$	$\pi^0 K_L^0 \pi^+ \pi^+ \pi^- K^-$	70	58	23768
19	$J/\psi \rightarrow \eta e \gamma, \eta e \rightarrow K^- p \bar{\Lambda}, \bar{\Lambda} \rightarrow \pi^+ \bar{p}$	$\pi^+ K^- p \bar{p} \gamma$	77	58	23826
20	$J/\psi \rightarrow \pi^+ \pi^- K^* \bar{K}^*, K^* \rightarrow \pi^0 K^0, \bar{K}^* \rightarrow \pi^+ K^-, K^0 \rightarrow K_L^0$	$\pi^0 K_L^0 \pi^+ \pi^+ \pi^- K^-$	73	56	23882
21	$J/\psi \rightarrow \pi^- \bar{K}^* K^{*+}, \bar{K}^* \rightarrow \pi^+ K^-, K^{*+} \rightarrow \pi^+ K^0, K^0 \rightarrow K_L^0$	$K_L^0 \pi^+ \pi^+ \pi^- K^-$	59	56	23938
22	$J/\psi \rightarrow \pi^+ \pi^+ \pi^- \pi^- K^+ K^-$	$\pi^+ \pi^+ \pi^- \pi^- K^+ K^-$	78	56	23994
23	$J/\psi \rightarrow K^- p \bar{\Lambda}, \bar{\Lambda} \rightarrow \pi^+ \bar{p}$	$\pi^+ K^- p \bar{p}$	72	54	24048
24	$J/\psi \rightarrow \pi^+ \pi^- K^{*+} K^{*-}, K^{*+} \rightarrow \pi^+ K^0, K^{*-} \rightarrow \pi^0 K^-, K^0 \rightarrow K_S^0, K_S^0 \rightarrow \pi^+ \pi^-$	$\pi^0 \pi^+ \pi^+ \pi^- \pi^- K^-$	104	49	24097
25	$J/\psi \rightarrow \rho^0 K^* \bar{K}^*, \rho^0 \rightarrow \pi^+ \pi^-, K^* \rightarrow \pi^- K^+, \bar{K}^* \rightarrow \pi^+ K^-$	$\pi^+ \pi^+ \pi^- \pi^- K^+ K^-$	92	47	24144

(09+12) Inc. MC
(Partial reconstruction)

(09+12) Inc. MC
(Full reconstruction)

$$N_{PeakingBKG}^{Scale} = N_{J/\psi}^{09+12} \cdot \varepsilon \cdot Br(J/\psi \rightarrow p K^- \bar{\Lambda}) \cdot Br(\bar{\Lambda} \rightarrow \bar{p} \pi^+) \sim 77$$

$$\bullet \quad \varepsilon = 2.13 \times 10^{-4}$$

The contribution from peak background $J/\psi \rightarrow p K^- \bar{\Lambda}$ that have been normalized into the data is negligible.

Systematic uncertainty of combined tracking and recons.-efficiency of Λ [II]

Peaking
background

Signal
channel

Table 1: Decay trees and their respective final states.

rowNo	decay tree	decay final state	iDcYTr	nEtr	nCEtr
1	$J/\psi \rightarrow K^+ \bar{p} \Sigma^0, \Sigma^0 \rightarrow \Lambda \gamma, \Lambda \rightarrow \pi^- p$	$\pi^- K^+ p \bar{p} \gamma$	1	30211	30211
2	$J/\psi \rightarrow K^+ \bar{p} \Sigma^0, \Sigma^0 \rightarrow \Lambda \gamma, \Lambda \rightarrow \pi^0 n$	$\pi^0 K^+ n \bar{p} \gamma$	0	21650	51861
3	$J/\psi \rightarrow K^+ \bar{p} \Lambda, \Lambda \rightarrow \pi^- p$	$\pi^- K^+ p \bar{p}$	2	2254	54115
4	$J/\psi \rightarrow \pi^+ \pi^- p \bar{p}$	$\pi^+ \pi^- p \bar{p}$	7	635	54750
5	$J/\psi \rightarrow \pi^+ p \bar{\Delta}^{--}, \bar{\Delta}^{--} \rightarrow \pi^- \bar{p}$	$\pi^+ \pi^- p \bar{p}$	6	327	55077
6	$J/\psi \rightarrow K^+ \bar{p} \Sigma^0, \Sigma^0 \rightarrow \Lambda \gamma, \Lambda \rightarrow \pi^0 n, \pi^0 \rightarrow e^+ e^- \gamma^F$	$e^+ e^- K^+ n \bar{p} \gamma^F \gamma$	17	206	55283
7	$J/\psi \rightarrow \pi^0 \pi^+ \pi^- p \bar{p}$	$\pi^0 \pi^+ \pi^- p \bar{p}$	13	164	55447
8	$J/\psi \rightarrow \pi^0 \Delta^{++} \bar{\Delta}^{--}, \Delta^{++} \rightarrow \pi^+ p, \bar{\Delta}^{--} \rightarrow \pi^- \bar{p}$	$\pi^0 \pi^+ \pi^- p \bar{p}$	20	136	55583
9	$J/\psi \rightarrow \pi^0 \Delta^+ \bar{\Delta}^-, \Delta^+ \rightarrow \pi^0 p, \bar{\Delta}^- \rightarrow \pi^0 \bar{p}$	$\pi^0 \pi^0 \pi^0 p \bar{p}$	38	125	55708
10	$J/\psi \rightarrow \pi^- \bar{p} \Delta^{++}, \Delta^{++} \rightarrow \pi^+ p$	$\pi^+ \pi^- p \bar{p}$	22	123	55831
11	$J/\psi \rightarrow \omega p \bar{p}, \omega \rightarrow \pi^0 \pi^+ \pi^-$	$\pi^0 \pi^+ \pi^- p \bar{p}$	18	110	55941
12	$J/\psi \rightarrow K^+ \bar{p} \Sigma^{*0}, \Sigma^{*0} \rightarrow \pi^0 \Lambda, \Lambda \rightarrow \pi^- p$	$\pi^0 \pi^- K^+ p \bar{p}$	14	109	56050
13	$J/\psi \rightarrow K^+ \bar{p} \Sigma^0, \Sigma^0 \rightarrow \Lambda \gamma, \Lambda \rightarrow n \gamma$	$K^+ n \bar{p} \gamma \gamma$	57	106	56156
14	$J/\psi \rightarrow \pi^+ \Delta^+ \bar{\Delta}^{--}, \Delta^+ \rightarrow \pi^0 p, \bar{\Delta}^{--} \rightarrow \pi^- \bar{p}$	$\pi^0 \pi^+ \pi^- p \bar{p}$	10	99	56255
15	$J/\psi \rightarrow \pi^+ \Delta^0 \bar{\Delta}^-, \Delta^0 \rightarrow \pi^- p$	$\pi^+ \pi^- p \bar{p}$	11	90	56345
16	$J/\psi \rightarrow \Delta^{++} \bar{\Delta}^{--}, \Delta^{++} \rightarrow \pi^+ p, \bar{\Delta}^{--} \rightarrow \pi^- \bar{p}$	$\pi^+ \pi^- p \bar{p}$	9	86	56431
17	$J/\psi \rightarrow \eta_c \gamma, \eta_c \rightarrow K^+ \bar{p} \Lambda, \Lambda \rightarrow \pi^- p$	$\pi^- K^+ p \bar{p} \gamma$	19	83	56514
18	$J/\psi \rightarrow \pi^0 \pi^+ n \bar{p}$	$\pi^0 \pi^+ n \bar{p}$	67	60	56574
19	$J/\psi \rightarrow \eta_c \gamma, \eta_c \rightarrow K^+ \bar{p} \Lambda, \Lambda \rightarrow \pi^0 n$	$\pi^0 K^+ n \bar{p} \gamma$	49	59	56633
20	$J/\psi \rightarrow \pi^- \bar{\Delta}^- \Delta^{++}, \bar{\Delta}^- \rightarrow \pi^0 \bar{p}, \Delta^{++} \rightarrow \pi^+ p$	$\pi^0 \pi^+ \pi^- p \bar{p}$	42	57	56690
21	$J/\psi \rightarrow \pi^0 \pi^0 p \bar{p}$	$\pi^0 \pi^0 p \bar{p}$	43	52	56742
22	$J/\psi \rightarrow \pi^0 \pi^+ \pi^- K^+ K^-$	$\pi^0 \pi^+ \pi^- K^+ K^-$	3	48	56790
23	$J/\psi \rightarrow \pi^- \bar{\Delta}^0 \Delta^+, \bar{\Delta}^0 \rightarrow \pi^+ \bar{p}$	$\pi^+ \pi^- p \bar{p}$	32	47	56837

Table 1: Decay trees and their respective final states.

rowNo	decay tree	decay final state	iDcYTr	nEtr	nCEtr
1	$J/\psi \rightarrow K^+ \bar{p} \Sigma^0, \Sigma^0 \rightarrow \Lambda \gamma, \Lambda \rightarrow \pi^- p$	$\pi^- K^+ p \bar{p} \gamma$	0	20105	20105
2	$J/\psi \rightarrow K^+ \bar{p} \Sigma^0, \Sigma^0 \rightarrow \Lambda \gamma, \Lambda \rightarrow \pi^0 n$	$\pi^0 K^+ n \bar{p} \gamma$	9	568	20673
3	$J/\psi \rightarrow \pi^0 \Delta^{++} \bar{\Delta}^{--}, \Delta^{++} \rightarrow \pi^+ p, \bar{\Delta}^{--} \rightarrow \pi^- \bar{p}$	$\pi^0 \pi^+ \pi^- p \bar{p}$	15	202	20875
4	$J/\psi \rightarrow \pi^0 \pi^+ \pi^- p \bar{p}$	$\pi^0 \pi^+ \pi^- p \bar{p}$	3	156	21031
5	$J/\psi \rightarrow \omega p \bar{p}, \omega \rightarrow \pi^0 \pi^+ \pi^-$	$\pi^0 \pi^+ \pi^- p \bar{p}$	23	146	21177
6	$J/\psi \rightarrow \pi^+ \pi^- p \bar{p}$	$\pi^+ \pi^- p \bar{p}$	10	131	21308
7	$J/\psi \rightarrow \pi^+ p \bar{\Delta}^{--}, \bar{\Delta}^{--} \rightarrow \pi^- \bar{p}$	$\pi^0 \pi^+ \pi^- p \bar{p}$	5	81	21389
8	$J/\psi \rightarrow \pi^+ p \bar{\Delta}^{--}, \bar{\Delta}^{--} \rightarrow \pi^- \bar{p}$	$\pi^+ \pi^- p \bar{p}$	30	66	21455
9	$J/\psi \rightarrow \pi^0 \pi^+ \pi^- K^+ K^-$	$\pi^0 \pi^+ \pi^- K^+ K^-$	8	52	21507
10	$J/\psi \rightarrow \pi^- \bar{\Delta}^- \Delta^{++}, \bar{\Delta}^- \rightarrow \pi^0 \bar{p}, \Delta^{++} \rightarrow \pi^+ p$	$\pi^0 \pi^+ \pi^- p \bar{p}$	26	50	21557
11	$J/\psi \rightarrow \eta_c \gamma, \eta_c \rightarrow K^+ \bar{p} \Lambda, \Lambda \rightarrow \pi^- p$	$\pi^- K^+ p \bar{p} \gamma$	17	48	21605
12	$J/\psi \rightarrow \pi^0 \pi^- \bar{K}^* K^{*+}, \bar{K}^* \rightarrow \pi^+ K^-, K^{*+} \rightarrow \pi^0 K^+$	$\pi^0 \pi^0 \pi^+ \pi^- K^+ K^-$	4	46	21651
13	$J/\psi \rightarrow \pi^- \bar{p} \Delta^{++}, \Delta^{++} \rightarrow \pi^+ p$	$\pi^+ \pi^- p \bar{p}$	29	44	21695
14	$J/\psi \rightarrow \rho^- \bar{K}^* K^{*+}, \rho^- \rightarrow \pi^0 \pi^-, \bar{K}^* \rightarrow \pi^+ K^-, K^{*+} \rightarrow \pi^0 K^+$	$\pi^0 \pi^0 \pi^+ \pi^- K^+ K^-$	67	43	21738
15	$J/\psi \rightarrow \Delta^{++} \bar{\Delta}^{--}, \Delta^{++} \rightarrow \pi^+ p, \bar{\Delta}^{--} \rightarrow \pi^- \bar{p}$	$\pi^+ \pi^- p \bar{p}$	79	42	21780
16	$J/\psi \rightarrow \rho^+ K^* K^{*-}, \rho^+ \rightarrow \pi^0 \pi^+, K^* \rightarrow \pi^- K^+, K^{*-} \rightarrow \pi^- \bar{K}^0, \bar{K}^0 \rightarrow K_L^0$	$\pi^0 K_L^0 \pi^+ \pi^- \pi^- K^+$	46	35	21815
17	$J/\psi \rightarrow K^+ \bar{p} \Lambda, \Lambda \rightarrow \pi^- p$	$\pi^- K^+ p \bar{p}$	74	33	21848
18	$J/\psi \rightarrow \rho^+ K^* K^{*-}, \rho^+ \rightarrow \pi^0 \pi^+, K^* \rightarrow \pi^- K^+, K^{*-} \rightarrow \pi^0 K^-$	$\pi^0 \pi^0 \pi^- \pi^- K^+ K^-$	7	31	21879
19	$J/\psi \rightarrow \pi^- \bar{K}^* K^{*+}, \bar{K}^* \rightarrow \pi^+ K^-, K^{*+} \rightarrow \pi^0 K^+$	$\pi^0 \pi^+ \pi^- K^+ K^-$	12	26	21905
20	$J/\psi \rightarrow \pi^+ \pi^- K^* \bar{K}^*, K^* \rightarrow \pi^- K^+, \bar{K}^* \rightarrow \pi^+ K^-$	$\pi^+ \pi^+ \pi^- \pi^- K^+ K^-$	14	25	21930
21	$J/\psi \rightarrow \pi^+ \pi^- \eta K^+ K^-, \eta \rightarrow \pi^0 \pi^0 \pi^0$	$\pi^0 \pi^0 \pi^0 \pi^+ \pi^- K^+ K^-$	100	23	21953
22	$J/\psi \rightarrow \pi^- \bar{\Delta}^0 \Delta^+, \bar{\Delta}^0 \rightarrow \pi^+ \bar{p}, \Delta^+ \rightarrow \pi^0 p$	$\pi^0 \pi^+ \pi^- p \bar{p}$	64	22	21975
23	$J/\psi \rightarrow \pi^+ \pi^- K^{*+} K^{*-}, K^{*+} \rightarrow \pi^0 K^+, K^{*-} \rightarrow \pi^- \bar{K}^0, \bar{K}^0 \rightarrow K_L^0$	$\pi^0 K_L^0 \pi^+ \pi^- \pi^- K^+$	71	21	21996

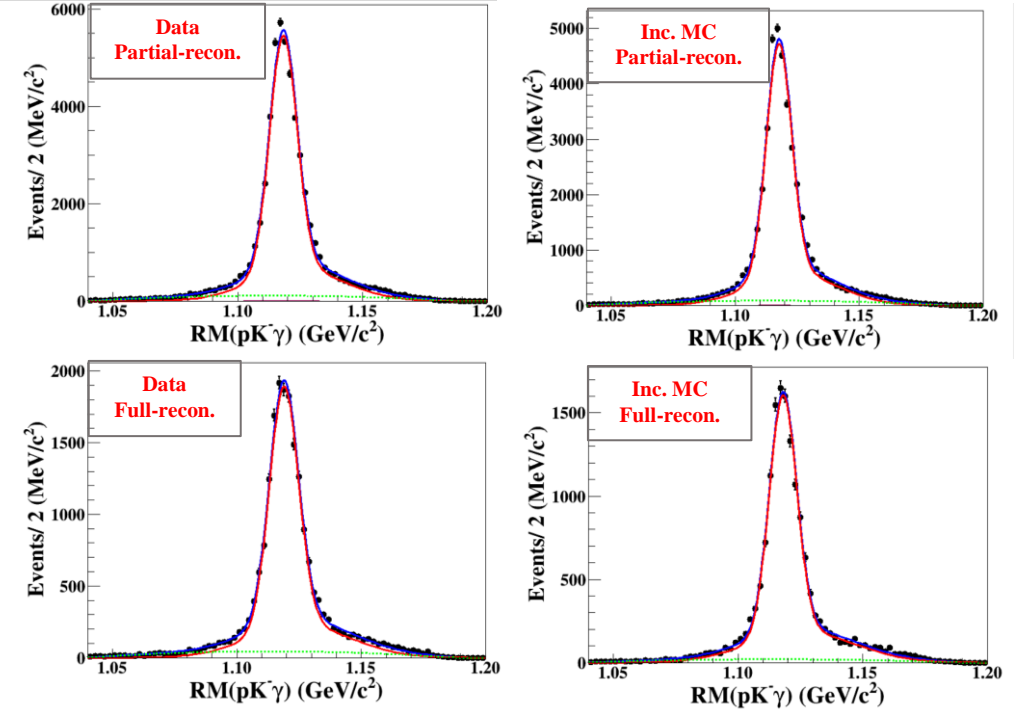
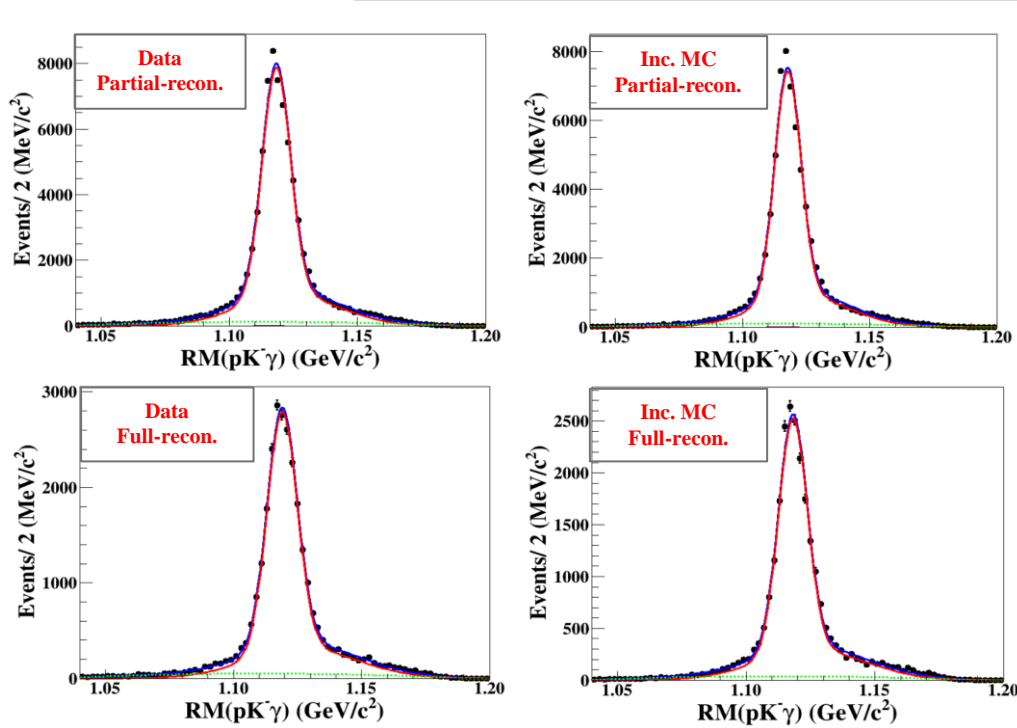
(18+19)/10. Inc. MC
(Partial reconstruction)

(18+19)/10. Inc. MC
(Full reconstruction)

The contribution from peak background $J/\psi \rightarrow \bar{p} K^+ \Lambda$ that have been normalized into the data is negligible.

Systematic uncertainty of combined tracking and recons.-efficiency of $\bar{\Lambda}(\text{II})$

control sample II: $J/\psi \rightarrow pK^-\bar{\Sigma}^0, \bar{\Sigma}^0 \rightarrow \gamma\bar{\Lambda}$



09+12

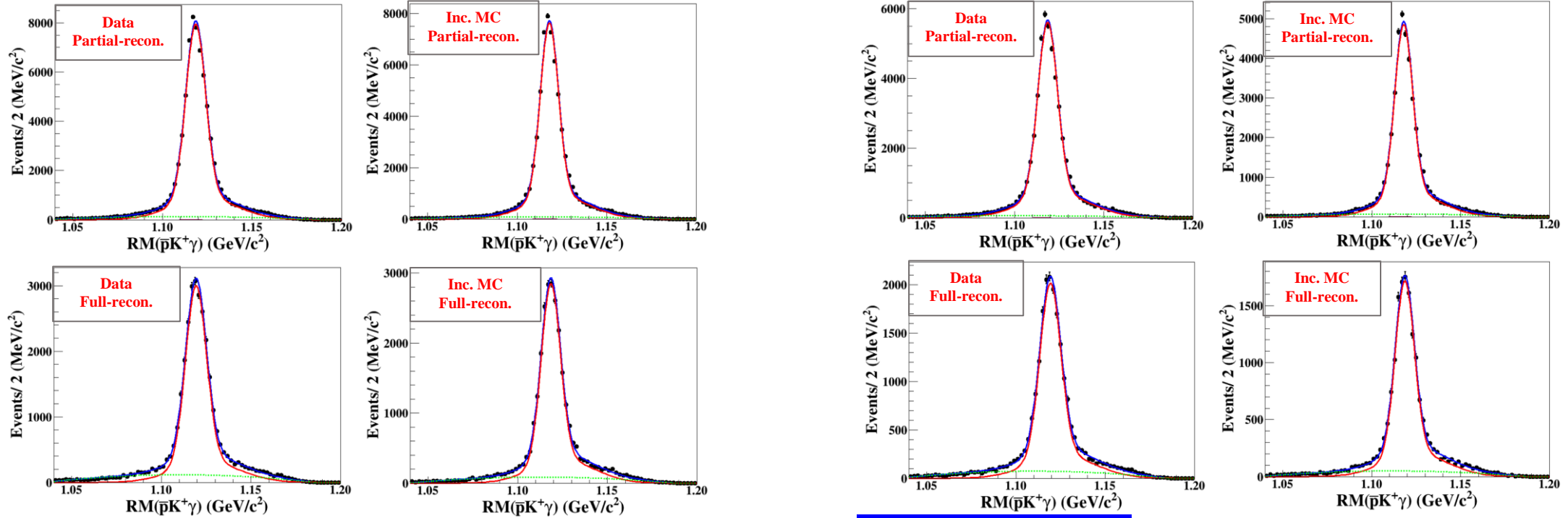
$\bar{\Lambda}$ reconstruction	Data(fit)	Inc. MC(fit)
$\text{RM}(pK^-\gamma)(N_{\text{chrg}} \geq 2)$	70835.7 ± 439.3	62784.9 ± 330.7
$\text{RM}(pK^-\gamma)(N_{\text{chrg}} \geq 4)$	26320.9 ± 266.0	23374.1 ± 216.1
Efficiency($\epsilon\%$)	59.13	58.26
$\Delta(\%)$	1.5	

(18+19)/10 to check

$\bar{\Lambda}$ reconstruction	Data	Inc. MC
$\text{RM}(pK^-\gamma)(N_{\text{chrg}} \geq 2)$	48161.0 ± 305.4	39245.2 ± 265.4
$\text{RM}(pK^-\gamma)(N_{\text{chrg}} \geq 4)$	17909.6 ± 195.6	14706.6 ± 186.7
Efficiency($\epsilon\%$)	58.20	58.64
$\Delta(\%)$	0.8	

Systematic uncertainty of combined tracking and recons.-efficiency of $\Lambda(\Pi)$

control sample II: $J/\psi \rightarrow \bar{p}K^+\Sigma^0, \Sigma^0 \rightarrow \gamma\Lambda$



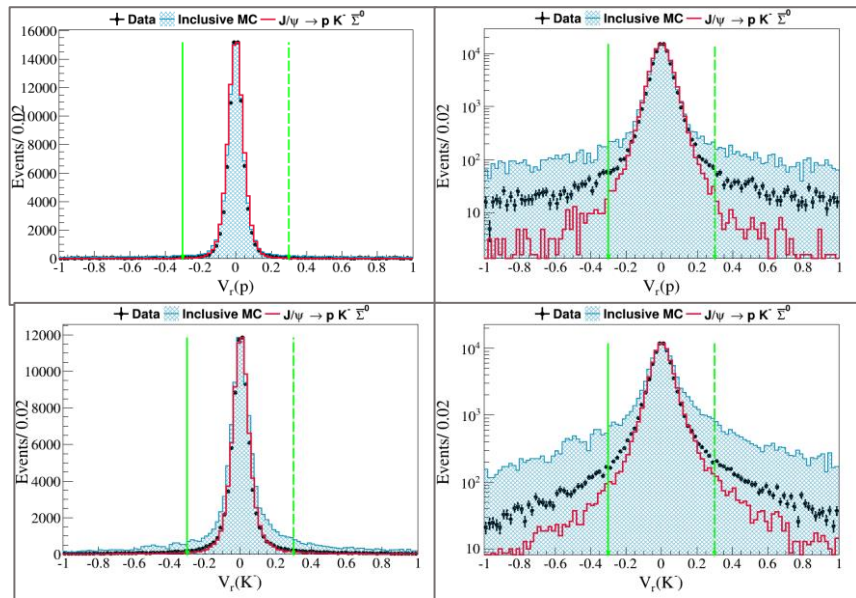
09+12

Λ reconstruction	Data	Inc. MC
$RM(\bar{p}K^+\gamma)(N_{\text{chrg}} \geq 2)$	69127.7 ± 326.2	62009.7 ± 296.6
$RM(\bar{p}K^+\gamma)(N_{\text{chrg}} \geq 4)$	26851.0 ± 263.9	24142.7 ± 215.4
Efficiency($\epsilon\%$)	60.79%	60.93%
$\Delta(\%)$	0.2	

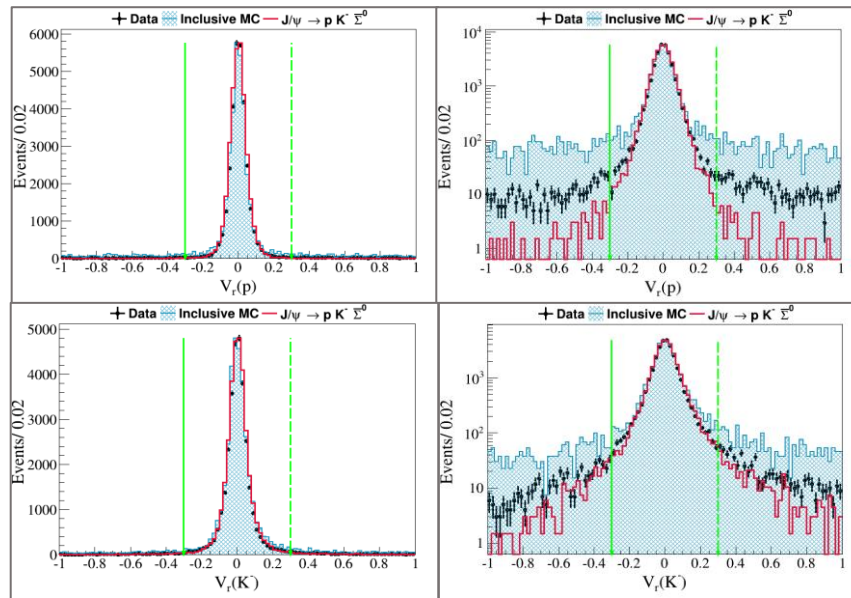
(18+19)/10 to check

Λ reconstruction	Data	Inc. MC
$RM(\bar{p}K^+\gamma)(N_{\text{chrg}} \geq 2)$	50204.4 ± 256.9	39250.4 ± 260.2
$RM(\bar{p}K^+\gamma)(N_{\text{chrg}} \geq 4)$	18600.4 ± 235.8	14809.1 ± 163.4
Efficiency($\epsilon\%$)	57.98%	59.05%
$\Delta(\%)$	1.8	

Partial-recon.



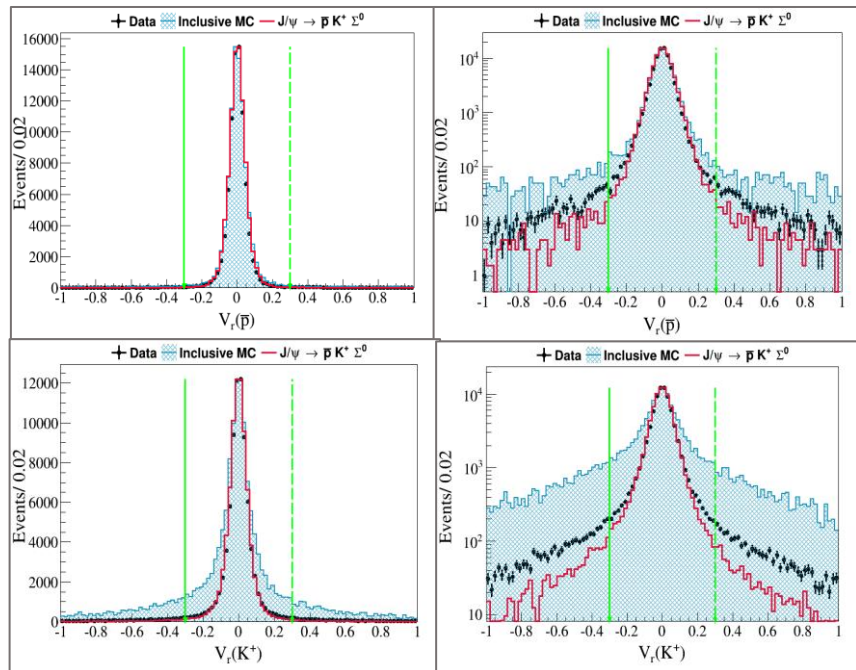
Full-recon.



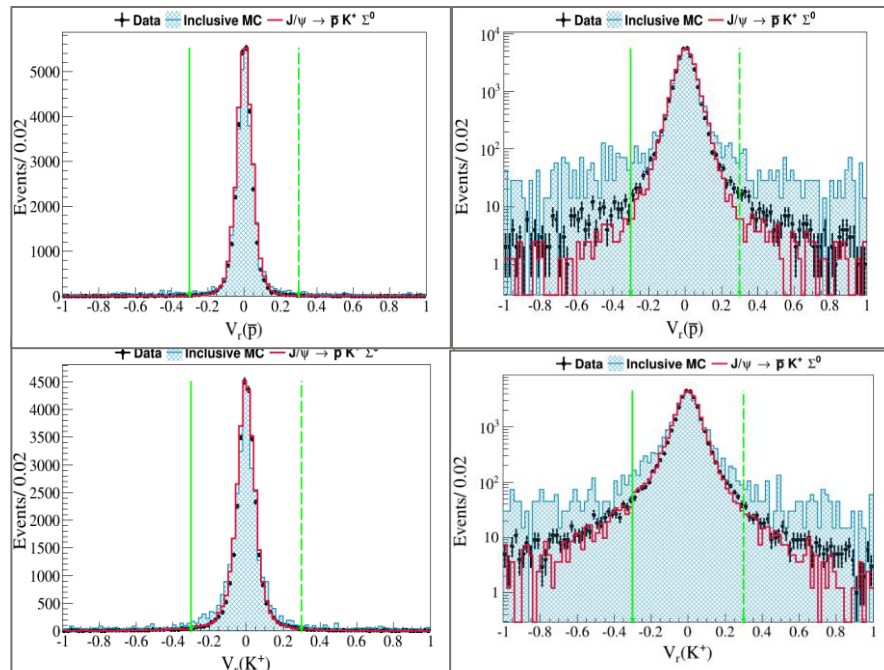
control sample:
 $J/\psi \rightarrow p K^- \bar{\Sigma}^0, \bar{\Sigma}^0 \rightarrow \gamma \bar{\Lambda}$

Systematic uncertainty of combined
tracking and recons.-efficiency of $\bar{\Lambda}$

Partial-recon.



Full-recon.



control sample:
 $J/\psi \rightarrow \bar{p} K^+ \Sigma^0, \Sigma^0 \rightarrow \gamma \Lambda$

Systematic uncertainty of combined
tracking and recons.-efficiency of Λ